A STUDY AND EVALUATION OF A METHOD FOR FORCASTING OCEAN SWELL WAVES USING WAVE SPECTRA

JOHN H. NEGELE, JR.
AND
JOHN L. BLONDIN

A STUDY AND EVALUATION OF A METHOD FOR FORECASTING OCEAN SWELL WAVES USING WAVE SPECTRA

* * * * * *

John H. Negele, Jr.

and

John L. Blondin

A STUDY AND EVALUATION OF A METHOD FOR FORECASTING OCEAN SWELL WAVES USING WAVE SPECTRA

by

John H. Negele, Jr.

Lieutenant, United States Navy

and

John L. Blondin

Lieutenant, United States Navy

Submitted in partial fulfillment of
the requirements for the degree of

MASTER OF SCIENCE
IN
AEROLOGY

United States Naval Postgraduate School
Monterey, California

1 9 5 7

A STUDY AND EVALUATION OF A METHOD FOR FORECASTING OCEAN SWELL WAVES USING WAVE SPECTRA

by

John H. Negele, Jr.

and

John L. Blondin

This work is accepted as fulfilling

the thesis requirements for the degree of

MASTER OF SCIENCE

IN

AEROLOGY

from the

United States Naval Postgraduate School

ABSTRACT

An investigation is made of the wave forecasting method of Pierson, Neumann and James of New York University, published as H. O. Pub. No. 603. The ocean "swell" spectral energy as predicted by the application of this forecast method is compared to the observed spectral energy present as estimated from ocean wave recording devices installed at the surface and at a depth of 80 feet, in the coastal waters off Davenport, California.

The comparison of the observed and forecast spectral energy for nine verification times taken at twelve hour intervals from 28 January 1954 to 1 February 1954 suggested the following conclusions:

1. For the conditions of the investigation, it was the opinion of the authors that the "swell" forecast was operationally useful.

2. The data of this investigation suggested the possibility that the forecast energy spectrum is too high in the low and middle frequencies and too low in the high frequency bands for high wind speeds.

3. The data of this investigation indicated that at certain verification times, energy reductions due to cross-sea interference were important.

The authors wish to express their appreciation for the advice and encouragement of Professor J. B. Wickham under whose direction this study was carried out.

Appreciation is also expressed to Professor R. L. Wiegel, of the Institute of Engineering Research, Berkeley, California, who made available the wave records upon which this study is based.

TABLE OF CONTENTS

Chapter	Title	Page
1.	Introduction	1
2.	The Theory and the Method	4
3.	The Forecast of the Energy Spectrum	11
4.	Spectrum Analysis	19
5.	Statement of Results	23
6.	Conclusions	27
	Bibliography	65
Appendix		
I	Tabled Values of $\overline{[A(f)]}^2$	67
II	Description of Locale and Facilities at Davenport, California	68
III	Description of the Synoptic Situation during and Preceding the Forecast Time	69

LIST OF ILLUSTRATIONS

Figure		Page
1.	Continuous Wave Spectrum for Fully Arisen Sea	34
2.	Wave Spectrum and Co-cumulative Spectrum (C.C.S.)	35
3.	C.C.S. Duration Graph	36
4.	C.C.S. Fetch Graph	37
5.	The Effect of Direction in the Filter	38
6.	Definition of Θ_3 and Θ_4	39
7.	Surface Synoptic Situation, 1230Z, 24 January 1954	40
8.	Surface Synoptic Situation, 0630Z, 27 January 1954	41
9A.	T_U and T_L as a Function of Time	42
9B.	Dispersion Envelope	43
10.	Forecast Spectral Energy Present at Davenport, California, at 0430Z, 28 January 1954	44
11.	Forecast Spectral Energy Present at Davenport, California, at 1630Z, 29 January 1954 (t_4)	45
12.	Variations of the Angular Spreading Factor in Different Portions of the Fetch	46
13.	Location of Recorders	47
14.	Comparison of E at Davenport, California	48
15.	Comparison of E at Davenport, California	49
16.	Comparison Time t_5	50
17.	Comparison Time t_7	51
18.	Mean Surface Chart, 1230Z, 25 January 1954 to 1230Z, 26 January 1954	52
19.	The Spectrum of the Cross-sea	53
20.	Variations of Wind Speed with Time	54
21.	Illustration of a Wave Record	55
22.	Comparison of Significant Wave Heights	56

Table		Page
1.	Wave Height Data as a Function of E	57
2.	Data Obtained from Synoptic Map	58
3.	Data Computed from Parameters of Table 2	60
4.	Beaufort Wind Speed	62
5.	Stability Factor	62
6.	Isobar Curvature Correction	62
7.	Reliability of Power Spectrum Estimates	63
8.	$[A(f)]^2$ as a Function of Wind Speed	64

TABLE OF SYMBOLS AND ABBREVIATIONS

Symbol or Abbreviation	Definition	Unit
N. Y. U. Method	New York University Forecast Method by Pierson, Neumann and James	
$[A(f)]^2\,df$	Spectral Wave Amplitude squared between the frequencies f and f $\neq$ df	ft^2-sec
π	3.1416	
f	Frequency - cycles per second	sec^{-1}
T	Wave period - $\frac{1}{f}$	sec
g	Acceleration of gravity	$ft\text{-}sec^{-2}$
V	Wind speed on ocean surface	$ft\text{-}sec^{-1}$ or knots
E	Area obtained by integrating $[A(f)]^2\,df$ over the range of frequencies between f_1 and f_2. Proportional to the total energy per unit surface area in a wave spectrum	ft^2
F	Fetch, area of the ocean of specified dimensions over which the wind is assumed to be constant	
C.C.S.	Co-Cumulative Spectrum	
G. V.	Group Velocity	knots
T_U	Highest period present at a given location	sec
T_L	Lowest period present at a given location	sec
θ_3, θ_4	Angles measured from the corners of the leeward side to the observation point (see Figure 6)	degrees
ETA	Estimated time of Arrival	hrs/date
T_s	Temperature of Sea Water	^oF
GCT, Z	Greenwich Civil Time	hrs/date
t_i	Forecast time	hrs/date
V_{gs}	Geostrophic Wind reduced to Ocean Surface	knots
V_g	Geostrophic Wind	knots

T_a	Temperature of Air	^oF
I_c	Isobar Curvature	miles^{-1}
I_{cc}	Isobar Curvature Correction	
V_{ob}	Wind Observed	knots
R_o	Distance from center of Fetch leeward to observation point	nautical miles
F_{LG}	Fetch Length	nautical miles
F_W	Fetch Width	nautical miles
F_L	Limiting Fetch	nautical miles
T_{ob}	Travel Time	hours
T_d	Duration Time, time the wind acted on Sea Surface	hours
T_E	Equivalent Duration	hours

CHAPTER 1

INTRODUCTION

The value of reliable techniques for forecasting ocean wave properties for seagoing and coastal operations, particularly military operations, is obvious.

This problem has engaged the interest and attention of some of the foremost scientists of various fields over the years. Some of the contributions have been notable.

The theories of classical hydrodynamics were applied by Lamb [1] in 1879, which yielded important properties of certain relatively simple sine-wave forms.

In 1933, Cornish[2], published the results of a large number of carefully made visual observations of wind-waves, both in deep water and near the shore, which were the first of that kind and which undoubtedly stimulated further work of this nature.

The development of continuous wave recording devices [3] expanded the wave data available and made possible the many statistical studies which have been carried out.

Sverdrup and Munk [4] published a wave forecasting method in 1947, for predicting the generation, decay, and transformation of the "significant" wind-waves.

Bretschneider, in 1951, published a modification forecast [5] of the Sverdrup and Munk technique based on more observational data.

In 1953, Pierson, Neumann and James of New York University published a new theory and corresponding forecast technique [6]. This theory and method are in many respects unique and depend largely on some assumptions which have had limited testing.

Since this last theory and technique has been adopted for use by the United States Naval Service, a study and evaluation of the method is the purpose of this paper. A study of this nature presents many difficulties and requires data and facilities available at very few institutions. These facts explain the paucity of published results of such studies. To the knowledge of the authors, no such studies and evaluations have been made previously of the Pierson, Neumann and James wave forecast method, henceforth referred to as the N. Y. U. method, for Pacific Ocean swell, although the waves forecast in a generating area have been studied [16].

The study divides itself naturally into four distinct phases:

1. A wave forecast for a given period of time at a specified location, using the N. Y. U. method.

2. The analysis of wave records from a wave recording device for the same location and same time to obtain the actual wave conditions.

3. The comparison of the forecast and observed wave properties.

4. The results or conclusions to be drawn from the comparison.

The data and facilities necessary to carry out this study are listed below with their sources:

1. A forecast location at which suitable wave records have been kept for a convenient period of time. The site chosen was Davenport, California, where the University of California, Berkeley, had a series of recording devices [7] installed from the period of Nov. 1952 to Dec. 1954. Wave records from Jan. 1954 to Feb. 1954 were made available to the authors for use during this study.

2. A rapid computing device for the analysis of the wave records [8] to obtain the distribution of wave energy as a function of frequency [9]. The U. S. Naval Postgraduate School is equipped with a JRC 102-A medium-

speed general-purpose electronic computer which was available for this purpose.

3. Synoptic surface weather maps for the period of and preceding the forecast time for the purpose of preparing the detailed wave forecast. Such maps were made available by the Department of Mechanical Engineering Wave Research Laboratory, University of California, Berkeley.

4. A submarine contour chart for the area adjacent to the forecast location. U. S. Coast and Geodetic Original Survey Sheet No. 5266 of 25 April 1935, was made available by the Hopkins Marine Station, Pacific Grove, California.

CHAPTER 2

THE THEORY AND THE METHOD

The objective of this chapter is to discuss the portions of the N. Y. U. Method [6] and theory which relate directly to this investigation.

2A The Spectrum of Wind-Generated Waves

The primary basis for this forecast method is the assumed distribution of ocean wave energy for a given wind speed as a function of wave frequency in a wind-wave generation area, or the energy spectrum. This distribution is represented mathematically by:

$$\left[A(f)\right]^2 = \frac{c}{(2\pi)^5 f^6} e^{-\frac{g^2}{2\pi^2 f^2 V^2}} \qquad (1)$$

Where c is a constant of proportionality and the other terms are defined on page VI. Figure 1 shows a plot of this function for wind speeds of 20, 30, and 40 knots, and tabulated values of $\left[A(f)\right]^2$ as a function of wind speed and frequency are given in Appendix I.

The form of this function was assumed by Neumann [10] based on theoretical considerations and empirical evidence. To a large measure, the accuracy of this method will be determined by how closely the assumed spectrum approximates the true spectrum. Such determination will be possible only as increased test results become available.

2A1 Energy in the Spectrum

The integral of Equation (1) for a given wind velocity with respect to frequency is proportional to the energy of the included spectral components. This measure of spectral energy, between the frequencies f_1 and f_2, is defined as E and is given by

$$E = \int_{f_1}^{f_2} \left[A\ (f)\right]^2 \ df \qquad (2)$$

and has the dimensions, length squared.

Well-tested statistical relationships [11] between E and wave heights have been demonstrated. These relationships are given in Table 1 and are used as a basis for all wave height determinations, E being the forecasted parameter.

2A2 Properties of the Spectrum

The wind-generated sea for a given wind speed is said to be fully developed when all possible wave components in the spectrum between $f = 0$ and $f = \infty$ are present with their maximum amounts of spectral energy. This state is reached only after the wind has blown for a sufficient length of time ("duration") and over a sufficiently long distance ("fetch").

If the wind duration or fetch is insufficient for the fully developed state, a lower energy level will result. The spectral components form in the high frequency end of the spectrum initially and the lower frequency components are added progressively and grow as the wind duration increases until full development occurs, providing the fetch is not limiting and the wind continues. One important feature of this theory shows the partially developed spectra for limiting conditions of fetch and duration for various wind speeds.

2A3 The Co-cumulative Spectrum

The energy spectrum is converted to a more convenient form by integrating it over the entire frequency range. This procedure is illustrated in Figure 2. It will be noted that the ordinate of the cumulative

integral can be read directly in values of E, which is proportional to all of the wave energy in spectral components equal to or greater than the abscissa, f. The functional relationships between energy, wind, duration and fetch may also be included on the cumulative spectrum.

Figure 3 and Figure 4 illustrate the N. Y. U. co-cumulative spectra given as functions of duration and fetch respectively for various wind speeds. These are the curves normally used in the N. Y. U. method.

2B The Wave Forecast in the Generating Area

The foregoing are required for forecasting the wave conditions in a wind-wave generating area. Knowing the wind speed, the wind duration, and the fetch length, the E-value and the range of wave periods with important energy may be obtained directly from the co-cumulative spectrum. The sea in the generating area has an irregular, short-crested, appearance as the spectral components randomly amplify and damp each other. The spectral components also move in a variety of directions, as the wind action is not uniform, but of varying strength and direction.

2C The "Swell" Forecast

When wind-generated waves leave the generating area, a transformation takes place in the appearance of the sea surface as the wind no longer acts on the wave form. As the various spectral component wave trains leave the wind area, the apparent waves become regular and long crested, and are termed "swell." When "swell" arrives at points distant from the generating area, the waves have only a fraction of the energy originally present in the fetch.

2C1 Assumed Processes Involved in Energy Reductions

Pierson, Neumann and James account for energy reductions at points distant from the fetch by two processes, namely

integral can be read directly in values of E, which is proportional to all of the wave energy in spectral components equal to or greater than the abscissa, f. The functional relationships between energy, wind, duration and fetch may also be included on the cumulative spectrum.

Figure 3 and Figure 4 illustrate the N. Y. U. co-cumulative spectra given as functions of duration and fetch respectively for various wind speeds. These are the curves normally used in the N. Y. U. method.

2B The Wave Forecast in the Generating Area

The foregoing are required for forecasting the wave conditions in a wind-wave generating area. Knowing the wind speed, the wind duration, and the fetch length, the E-value and the range of wave periods with important energy may be obtained directly from the co-cumulative spectrum. The sea in the generating area has an irregular, short-crested, appearance as the spectral components randomly amplify and damp each other. The spectral components also move in a variety of directions, as the wind action is not uniform, but of varying strength and direction.

2C The "Swell" Forecast

When wind-generated waves leave the generating area, a transformation takes place in the appearance of the sea surface as the wind no longer acts on the wave form. As the various spectral component wave trains leave the wind area, the apparent waves become regular and long crested, and are termed "swell." When "swell" arrives at points distant from the generating area, the waves have only a fraction of the energy originally present in the fetch.

2C1 Assumed Processes Involved in Energy Reductions

Pierson, Neumann and James account for energy reductions at points distant from the fetch by two processes, namely

1. Dispersion

2. Angular Spreading

2C2 Dispersion

When the spectral components leave a generating area, the associated energy front of each travels at different group velocity. The group velocity for any spectral frequency is given by

$$G.\ V. = 1.515\ T \qquad (3)$$

Dispersion, then, is defined to be "the spreading-out effect caused by the different group velocities of the spectral frequencies in the original disturbance at the source." [6] Therefore, to determine for a given time the total spectral energy at a specified distance from the fetch, based on the effects of dispersion, it is necessary to compute the range of frequencies which could be present at that time. This may be accomplished by considering the distance the energy must travel, the group velocity, and the time the particular spectral component was formed as a function of wind speed, duration, and fetch.

The N. Y. U. method includes some basic "filters" which are essentially pre-arranged formulations of these variables, for certain recurring situations. The use of these "filters" permits the calculation of a T_U, upper period, and T_L, lower period. T_U and T_L define the upper and lower limits of the spectral energy present at the forecast time and location, for a given wind speed.

2C3 Angular Spreading

The considerations of paragraph 2C2 do not take into account the effect of variability in the direction of wave motion and the fact that the waves are short-crested. The component wave trains vary not only in frequency but also in direction within the area of generation. Thus, as

the spectral components leave the generating area, they spread out angularly as well as "disperse."

The assumed distribution of relative wave energy as a function of direction is illustrated in the lower curve of Figure 5. Since the area under this curve is unity, when integrated cumulatively over direction it gives that fraction of the energy to be found between any two directions (measured from that of the mean wind). The ordinate of the upper curve in Figure 5 is then expressable in percent. Dispersion and angular spreading computations are illustrated in chapter 3.-

Figure 6 illustrates the measurement of the angles θ_4 and θ_3, which are the parameters used in conjunction with the upper curve of Figure 5 for evaluating the effect of angular spreading. The convention adopted for measuring θ_4 and θ_3 is that clockwise angles are positive and counter-clockwise angles are negative.

The difference between the percentages obtained by entering the upper curve of Figure 5 with θ_4 and θ_3 is the percentage within that range of angles of the spectral energy computed from the dispersion envelope and the energy spectrum.

The bell-shaped distribution of energy with direction, Figure 5, was inferred from limited evidence [12] and to the knowledge of the authors, its exact form has had limited observational verification.

2C4 Other Sources of Possible Energy Loss

Pierson, Neumann and James [6] have stated that in many cases, dispersion and angular spreading are the only mechanisms necessary to account for the energy decrease observed in wave spectra at locations remote from the generating area. They held that there may be important

energy lost due to the effect of cross-sea interference,[1] but have expressed the opinion that losses due to viscosity are generally negligible. The effects of cross and opposing winds on wind-generated swell are not known, but undoubtedly would modify the spectrum of the swell to an extent dependent on the wind speed and the spectral composition of the cross-sea. It is believed that at least a qualitative evaluation of these effects will be possible as the volume of test results become greater.

The direct measurement of attenuation presents serious difficulties. However, a careful analysis of the actual spectral energy at a wave recorder as compared to the forecast spectral energy may indicate the presence of processes which cause energy losses. For instance, theory indicates that viscosity effects, if they are important at all, reduce the energy primarily in the high frequency end of the spectrum [8]. If high frequency energy from a distant fetch is forecast to arrive at a wave recorder at a given time, and fails to arrive, it might be inferred that viscosity effects were responsible for the energy loss. This possibility is discussed further in Chapter 6.

205 Goals of the Investigation

The goal of this paper is to make available the results of the comparison of the spectral energy forecast by the N. Y. U. method and the spectral energy as obtained from a wave-recording device.

[1] The assumed effect of cross-sea interference is that the swell with spectral components of the same frequency as the cross-sea wave trains will form unstable interference patterns with the latter. This will result in attenuation of the swell having spectral energy in those frequencies.

It was intended that these results would permit conclusions particularly in the following areas:

1. The assumed form of the energy spectrum.

2. The assumed form of the wave-energy directional spectrum.

3. The effects of viscosity and cross-seas on the spectrum of the swell waves.

4. A general verification of the system which implicitly includes the items above.

CHAPTER 3

THE FORECAST OF THE ENERGY SPECTRUM

This chapter contains a brief summary of the procedures followed by the authors in preparing a forecast of the energy spectrum for a given observation time.

When a breeze comes up, the sea surface instantaneously becomes covered with tiny ripples which form more or less regular arcs of long radius. They increase rapidly in height as energy is transferred to the waves by the pushing and dragging forces of the wind. Soon a state of irregular composite wave motion, called the sea, exists. The fully developed state over a long fetch with a sufficiently long duration finally will be attained when the wave-generating tractions have increased the total wave energy to such a point that dissipation balances the work done by pushing and dragging forces on the sea surface. The total amount of wave energy accumulated in the composite wave motion is now distributed over a wide range of frequencies. The curves and assumptions of the N. Y. U. method were used in forecasting the energy spectra in the fetch area. H. O. 603 contains several filters that can be applied to account for the reduction in the energy spectrum as its components move from the fetch area to an observation point. The authors, after considerable investigation and study, concluded that the idealized filters in H. O. 603 would not be convenient for use in this study. To achieve the desired results, a new method of solving for dispersion and angular spreading was devised. The new filter used when solving for the effects of dispersion allowed for wind variations in the fetch and resulted in a continuous dispersion envelope of periods present at the forecast point. The angular spreading factor allowed for any orientation of the fetch.

3A Selection of Data

Appendix II describes the elaborate instrumentation used by the University of California to record continuously the water level at Davenport, California. An examination of the wave records available showed that the average wave heights were higher in the winter at Davenport due to well-developed storms in the North Pacific area. Therefore, the months of January, February, and March 1954 were selected for closer study.

Weather maps at six-hour intervals were then studied for these three months. All possible wind circulations that resulted in fetches acting with components toward Davenport were recorded. An envelope showing the periods (T_U and T_L) and their estimated times of arrival (ETA) was computed for each fetch. These data (T_U, T_L, ETA) were tabled and plotted.[1] After detailed examination, the period between 0630Z, 23 January 1954 and 0430Z, 1 February 1954 was selected for thorough investigation and study.

This time interval was the most favorable for the following reasons:

1. A stationary nearly uniform fetch prevailed. It is discussed in Appendix III and illustrated in Figures 7 and 8.

2. Representative wave records were available in "fast time"[2] with a time interval of twelve hours, as explained in Appendix II.

3. Fetches A and B[3] contained weather station ship "P." "P" is manned by experienced aerographers. Therefore, its weather reports were assumed accurate. "P" also reports sea-water temperature (T_S) which

[1] Figure 9A is an example of this from 0630Z, 23 January 1954 to 0430Z, 1 February 1954.

[2] "Fast Time" is used to indicate the portions of the record where sea level was recorded on the scale of 6 inches per 1 minute.

[3] See Appendix III.

could be used in computing the stability factor,[1] which is used in estimating the wind speed.

4. Only fetches A, B, and C, as defined in Appendix III and illustrated in Figures 7 and 8, were believed to be producing significant energy at Davenport.

5. Local winds in the vicinity of Davenport were blowing from the land toward the sea and were light.

6. All instruments were cleaned and calibrated on 24 January 1954 and assumed to be in good working order.

Considerations 1, 2, and 4 established wave forecast times at Davenport which are as follows:

t_1 0430Z 28 Jan 1954

t_2 1630Z 28 Jan 1954

t_3 0430Z 29 Jan 1954

t_4 1630Z 29 Jan 1954

t_5 0430Z 30 Jan 1954

t_6 1630Z 30 Jan 1954

t_7 0430Z 31 Jan 1954

t_8 1630Z 31 Jan 1954

t_9 0430Z 1 Feb 1954

Hereafter, the forecast time will be referred to as t_i.

3B Compilation of Data

Table 2 records the data measured from the weather charts illustrated in Figure 7.

[1]See Table 5.

Table 3 records the data computed from parameters listed in Table 2 by the following procedures (symbols are all defined in Tables 2 and 3):

1. Stability Factor (V_{gs}/V_g) depends on T_s minus T_a and is determined from Table 5.

2. Isobar curvature correction (I_{cc}) depends on isobar curvature (I_c) and stability factor and is determined from Table 6.

3. Geostrophic wind reduced to sea surface (V_{gs})

$$V_{gs} = (Vg)\ (I_{cc})\ (\text{stability factor}) \qquad (4)$$

4. Surface wind speed (V) obtained by comparing V_{ob}, the reported surface wind, with V_{gs}.

5. Limiting fetch (F_L), upper period (T_U), and E were read directly from Figure 4 using V.

6. Equivalent duration (T_E) was established by comparing generation time of last V to present V, for an equal E-value.

7. Travel time (T_{ob})

$$T_{ob} = \frac{R_o \neq F_{LG} - F_L}{1.515\ T_U} \qquad (5)$$

Where T_U leaves the wind area from near the windward side of the fetch.[1]

8. Lower period (T_L)

$$T_L = \frac{R_o}{1.515\ T_{ob}} \qquad (6)$$

This T_L will have the same ETA as T_U because it left from the leeward side of the fetch.

9. Duration time (T_d)

$$T_d = T_E \neq \Delta T \qquad (7)$$

Where ΔT = 6 hours, or map interval.

[1]See Figure 7

10. Estimated time of arrival (ETA)

$$ETA = \text{map time} + T_{ob} \qquad (8)$$

3C Development of the Filter

The values of E^1 must be reduced by filters as the spectral components move from the generating area to the observation point. Chapter 2 explained the theory of filters involved in the N. Y. U. method. Two processes act to limit the energy at the observation point: dispersion and angular spreading.

3D Dispersion

Dispersion results from the presence of different group velocities among the spectral components in the fetch. The writers, to accurately account for the effects of dispersion, plotted T_U and T_L as a function of time.[2] T_U left from the windward side of the fetch with $R_o + F_{LG} - F_L$ distance to travel. T_L moved out of the leeward side with distance R_o to travel. Only periods between T_U and T_L were theoretically present at Davenport because of the dispersion influence.

Fetches A, B, and C were fully-developed wave generating areas; consequently, upper period waves (T_U) were also leaving from the leeward side with travel distance R_o. Their ETA was computed by

$$T_{ob} = \frac{R_o}{1.515\ T_U} \qquad (9)$$

and Equation (8). Due to a shorter travel distance this T_U arrived ahead of a similar T_U which left from fetch windward.

[1] See Table 3

[2] See Table 9A

To include the first arriving waves from the generating area, the waves created as the wind continued and the waves leaving the fetch area when the wind ceased, Figure 9A was modified into Figure 9B, a dispersion envelope. A dispersion envelope is a plot of T_U and T_L present from the same fetch as a function of the same ETA. The envelope was plotted from values obtained through the use of Figure 4 and Equations (5), (6), (8), and (9). The results are shown in Figure 9B which illustrates the various limiting envelopes of periods due to dispersion affecting Davenport before and during the forecast periods from fetches A, B, and C.

The resulting reduction in E due to dispersion is illustrated in Figure 10 for t_1 and Figure 11 for t_4.

3E Angular Spreading

Angular spreading results from the variability in wave direction in and after leaving the fetch area. The angular spreading factor is related to the orientation of the observation point with respect to the generating area and is therefore dependent upon the parameters θ_{3L}, θ_{4L}, θ_{3W}, and θ_{4W},[1] which were measured from the synoptic weather chart. For times near the end of a fetch life, important wave energy may come from the rear of the fetch (fetch windward). At these times the angular spreading factor decreases in value, consequently, less energy will be forecast to arrive.

The factors for the fetch leeward and fetch windward were obtained from an angular spreading factor graph.[2] The difference between these two factors was (from leeward to windward) as great as 20%. The authors considered the possible error introduced by using an angular spreading

[1] See Figure 7
[2] See Figure 5

factor averaged over the entire fetch as unacceptable. To accurately determine the angular spreading value as a function of distance from the fetch front, Equation (10) was used.

$$\Delta D = 1.515 (T_{ob}) T - R_o \qquad (10)$$

ΔD is the distance in nautical miles measured from the leeward side of the fetch into the generating area.[1]

T_{ob} is the travel time.

T is any period between T_U and T_L for t_i as determined by the dispersion envelope.

R_o is the distance from observation point to the center of fetch leeward.

In Equation (10), T was replaced by 1/frequency, a ΔD was computed for each 0.005 change in frequency for each t_i involving fetches A, B, and C. The distance, ΔD was then calculated and plotted, and a corresponding Θ_3 and Θ_4 measured. These angles, applied to the angular spreading graph, yielded the angular spreading factor. This procedure was used when it was evident that the waves were not leaving from the front of the fetch.

The resulting reduction in E due to angular spreading is shown in Figure 10 for t_1 and Figure 11 for t_4.

It is considered significant that the use of Equation (10) allowed for variations in angular spreading due to variations in ($R_o \neq \Delta D$). Figure 12 is a graph of angular spreading factor with respect to ΔD, for fetch A. This factor did not decrease at a constant rate in going from fetch leeward to fetch windward. Graphs, not included here, yielded similar results for fetches B and C. These variations in rate of change of the angular spreading factor depend upon the orientation of the various fetches with respect to Davenport.

[1]See Figure 7

3F Shallow Water Effects

Shallow water effects of refraction, shoaling, percolation, diffraction, and friction influence E as the deep water wave energy approaches the Davonport area.

Refraction was determined using the method presented in H. O. 234, and a wave refraction diagram constructed using U. S. Coast and Geodetic Original Survey Sheet No. 5266 of 25 April 1935. The chart shows the bottom contours seaward of Davenport to be nearly straight and parallel. The range of deep water wave directions was very small, therefore refraction was treated as if all deep water waves arrivod from one angle. Shoaling effects were also obtained from H. O. 234, Plate I.

Percolation and friction were assumed negligible due to the narrow width of the continental shelf. Diffraction was assumed to be negligible. All instruments were located in open water well away from rock formations or man-made structures.

The shallow-water effects of refraction and shoaling were combined into one correction factor. Their influence on E is shown in Figure 10 for t_1 and Figure 11 for t_4. Figures 10 and 11 show the resultant ocean wave spectral energy forecast to arrive at the recording instruments for t_1 and t_4. The area under the curve can be integrated by a planimeter to evaluate the total energy present for any forecast time. The results are shown in chapter 5, and are plotted with respect to time in Figure 14.

CHAPTER 4

SPECTRUM ANALYSIS

The objective of this chapter is to discuss the general procedure and theory employed in obtaining the energy spectrum from the record of a wave-recording device.

In this study, wave records were used from both a surface wave recording device and a pressure recording device.[1] The distinction between the two is that the former records surface waves and the latter records wave pressures at the depth in which it is installed.

4A Theory

Many of the features of surface, and below surface waves have been explained by Pierson and Marks [8] and Neumann [13] based on the assumption that a wave record as a function of time is the result of a Gaussian process. The theory was developed by Tukey and Hamming [9] among others. In the publication cited, the latter explain a method which may be used for estimating the power spectrum of a steady-state sea surface using the Fourier transform of the autocorrelation function. A text which treats correlation functions and power spectra in detail is Information Theory [17] by Goldman.

Timme and Stinson [14] present curves of the pressure response factor as a function of wave period, T, and depth, H. The pressure response factor is a measure of the attenuation of wave energy with depth.

4A1 Numerical Estimation of Non-normalized Autocorrelation Function and the Pressure Power Spectrum

The results of Tukey and Hamming [9] are used to derive the power

[1] See Appendix III

spectrum from a pressure record placed at the sea floor in a depth of water, H. The possible errors which enter into the numerical analysis have been considered. The corrections which must be applied to the raw results and the degree of reliability have been determined.

The formulas for numerical estimation of the power spectra as presented by Tukey and Hamming[9] and as used by Pierson and Marks [8] are given by:

$$t_2 - t_1, = t_3 - t_2 = \text{----} \; t_N - t_{N-1} = \Delta t \tag{11}$$

$$Q_p = \frac{2}{N-P} \sum_{n=1}^{N-P} P(t_n)\, P(t_{n-p}) \quad (P=0,1,2, \text{----} \; m) \tag{12}$$

$$L_h = \frac{1}{m} \left(Qo + 2 \sum_{P=1}^{m-1} Qp \cos \frac{\pi P h}{m} + Qm \cos \pi h\right) \tag{13}$$

$$(h=0,1,\text{---}m)$$

$$U_h = .23 L_{h-1} + .54 L_h + .23 L_{h+1} \quad (h=0,1, \text{---}m) \tag{14}$$

$$\mu_h = \frac{\pi h}{\Delta tm} \tag{15}$$

$$\left[A_{ph}(\mu_h)\right]^2 = \frac{U_h \Delta t m}{\pi} \tag{16}$$

Where $\mu = 2\pi f$

Equation (11) states that N-1 equally spaced time intervals are marked off on the record by points spaced Δt units apart. The values of pressure at these points in terms of departures from the mean are then tabulated as $P(t_1)$, $P(t_2)$ ---- $P(t_n)$, ---- $P(t_N)$, N numbers resulting.

The non-normalized lag coefficients are then found by the use of Equation (12). Q_p ranges from Q_o to Q_m, or m + 1 total numbers. Q_o is the E_{ph} max, or the total spectral energy uncorrected for the scale factor

of the record, at the depth H.

The summation of Equation (12) was accomplished by the use of a CRC-102-A computer.[1]

The "raw" estimates of power in the μ band from $\mu = \frac{\pi(h-\frac{1}{2})}{\Delta tm}$ to $\mu = \frac{\pi(h+\frac{1}{2})}{\Delta tm}$ are found from Equation (13). A plot of the "raw" estimates with values of h result in a quite jagged graph. The jaggedness is introduced by the measurement of P at discrete points and by the finite length of the record. A smoothing device is given by Equation (14).

The final number, U_h, is an estimate of the mean value of the power system from $\frac{\pi(h-\frac{1}{2})}{\Delta tm}$ to $\frac{\pi(h+\frac{1}{2})}{\Delta tm}$. At the point given by Equation (15) the best estimate of the value of $\left[A_{ph}(U_h)\right]^2$ is given by Equation (16). The result is a smoothing of the "jagged" curve of Equation (13), and this continuous curve is the best estimate of the pressure power spectrum.

For the purposes of this investigation, the computer program for the Fourier analysis was limited to Equation (13). The refinements, Equations (14), (15), (16) were not included in the solution, therefore, the resulting spectra are the "raw" or unsmoothed curves. This limitation was dictated by time considerations as the preparation of such a program is extremely longthy. These refinements will be included in the computer program as time permits and will be available for similar investigations in the future.

4A2 Reliability of Results

The final results of paragraph 4A1 are estimates. Estimates can be in error, and the important part of this analytical method is that it also presents an estimate of the error. Tukey and Hamming [9] have shown

[1]The computer programming of the equations used in this investigation was accomplished by Professors J. B. Wickham and H. H. Martinez of the U. S. Naval Postgraduate School.

that the errors follow a χ^2 distribution with f degrees of freedom given by

$$f = \frac{N - \frac{1}{2}m}{\frac{1}{2}m} \qquad (17)$$

Given f, then the use of Table (7) yields information on the reliability of the estimate for each frequency band obtained by the analysis.

For 20 degrees of freedom, the U_h obtained from Equation (16) may be multiplied by 1.8 and by .63. The true value of U in the band under analysis will lie between $1.8U_h$ and $.63U_h$ 90% of the time.

4B Procedure

For this investigation, the verification periods were of the order of twenty minutes on the wave record. The Δt was chosen as two seconds as determined by the criterion of Pierson and Marks [8]. The total number of measurements per wave record, N, was of the order of 600. For programming convenience, the total number of lags, m, was taken as 43.[1]

The total number of consecutive verifications, 12 hours apart, was nine.[2] It was originally intended that an autocorrelation program and a Fourier analysis would be carried out for each of these times. However, some initial difficulties in the programming routine restricted the time available for the investigation, and time did not permit the fulfillment of this objective.

[1] In future work, the wave record should be analyzed over a longer time interval resulting in greater value of N. This will increase the degrees of freedom and permit better resolution of the spectral curve. The number of lags taken should be increased.

[2] See pp 13, Chapter 3.

CHAPTER 5

STATEMENT OF RESULTS

The purpose of this chapter is to present the results of this investigation.

5A The "Filter"

It is the opinion of the authors that the "filter" devised for the energy spectra forecast in this study represents an accurate, practical method of solution. This is particularly true for the case of marked variation of wind speed with time in a generating area. For example, in the case of increasing wind speed with time, energy fronts generated by the earlier, lower speed winds will frequently be overtaken by energy fronts generated by the later, higher speed winds. This additional energy, from the higher speed wind might be overlooked if a plot of the "dispersion envelope" with time were not maintained.[1]

The filters and examples described in the N. Y. U. method 6 primarily treat the simplified cases of constant or slowly changing wind speed. This permits the energy to be obtained directly from the C.C.S. curves for one wind speed.

It must be understood that the "period envelope" must be identified precisely with the wind speed which generated it. It appears that the filter herein described[2] adequately handles the more complicated situations.

It appears that in forecasting by this method, using the filter presented herein, the forecaster will frequently need to work directly with the spectral curves in addition to the C.C.S. curves. For this

[1] See Figure 9B
[2] See Chapter 3

reason, the tabled solution to Equation (1) is included in Appendix I. It is recommended that personnel using this method plot the curves of the spectra for various wind speeds on an enlarged scale for the purpose of representing the spectrum present at the locality and time of interest.

5B Verification of the Forecast

Spectrum forecasts were prepared for Davenport, California, for the times t_1 through t_9 as described in Chapter 3. These forecasts were prepared for two geographical sites[1] having water depths of 50 and 81.5 feet respectively. A description of these sites and the instrumentation of each is presented in Appendix II.

Data available for verification of these forecasts were the following:

1. Significant wave height measurements for the sea surface, water depth 50 feet, hereafter called site I. These data were computed from sea surface wave records by personnel of the University of California, Berkeley, and made available to the authors for this study. Significant wave height, $H_{\frac{1}{3}}$, is defined as the average of the heights of the one-third highest waves. E values may be recovered by the statistical relationship,

$$H_{\frac{1}{3}} = 2.83\sqrt{E} \qquad (18)$$

A plot of the E values obtained in this manner for the times t_1 through t_9 is illustrated in Figure 14.

2. A sea-level wave record for site I obtained from a Beach Erosion Board, Step-resistor gauge as described in Appendix II. These records were analyzed by the procedures described in Chapter 4, and an estimate

[1]See Figure 13.

of the E value for times t_1 and t_2 were obtained.

3. A "pressure" record for the site in the water depth of 81.5 feet. This site will be referred to as site II. This pressure record was obtained from a Mark IX pressure-head instrument described in Appendix II. The instrument was installed $1\frac{1}{2}$ feet from the bottom at site II or in a water depth of approximately 80 feet. These records were analyzed by the procedures described in chapter 4 and an estimate of the E-value for times t_3 through t_9 were obtained.

As described above, the "records" available were obtained from two different instruments. For the times t_1 and t_2, the surface step-resistance device was available at site I. For the times t_3 through t_9 the pressure-head device, installed at a depth of 80 feet, was available at site II.

Figure 14 is a plot of E-values for the times t_1 through t_9 for the sea surface at site I, as estimated by:

1. The forecast.

2. The $H_{\frac{1}{3}}$ computations provided by the University of California, as described above. The 90% confidence limits [6] are plotted at each point.

3. The writers' analysis of the water level record of the step-resistance gauge as described above. The 90% confidence limits for these points are also included.[1]

Figure 15 is a plot of E-values for the times t_3 through t_9 for site II for a depth of 80 feet, as estimated by:

1. The forecast.

[1]See pp 22, Chapter 4.

2. The writers' analysis of the "pressure" record of the instrument as described above. The 90% confidence limits for these points are also included.[1]

The procedure for obtaining the forecast spectra and E-values for verification times t_3 through t_9 at site II was the following.
A surface spectrum forecast for a given verification was prepared at site II. This spectrum was reduced to a depth of 80 feet using the pressure response attenuation factors of Timme and Stinson [14] as described in Chapter 4. An example of the results of such a procedure is illustrated in Figures 16 and 17 for verification times t_5 and t_7 respectively.

As stated earlier, the original intention was to obtain the computed spectrum for each verification time. However, because of some initial difficulties encountered in the computer programs discussed in Chapter 4, the time allotted for the use of the computer did not permit the fulfillment of this objective.

A discussion of the figures described above, and the conclusions of the authors will be presented in Chapter 6.

[1]See pp 22, Chapter 4.

CHAPTER 6

CONCLUSIONS

The purpose of this chapter is to compare the observations with the forecasts and to suggest possible explanations for any differences noted.

6A General Comments on the Results

An examination of Figures 14 and 15, which compare forecast and observed energy, and Figure 22, which compares the forecast and observed significant height, indicates certain interesting features.

1. It is noted that the general agreement is quite good. The forecast energy peaks occurred at the time predicted and the energy was of the correct order of magnitude.

2. The forecast energy was in general equal to or greater than the observed.

3. At the point of greatest difference the forecast significant height was about one and one-half feet greater than the observed. This would indicate that for these conditions, the forecast would be of operational value.

4. It is noted that the points of closest agreement occur where the observed energy is at or near a peak.

6B Possible Explanations for the Differences between the Observed and Forecast Energy

For the purpose of suggesting possible explanations of differences between the observed and forecast energy, the following items are considered to be possible sources of error:

1. The theory. The forecast energy depends upon

   a. the energy spectrum and,

   b. the directional spectrum.

If the assumed form of either of these curves is incorrect, the energy forecast would probably be in error.

2. The application. In applying the method, it is unavoidable that the selection of data is largely subjective. It is possible therefore that sizable errors could be introduced. Errors in the following might be particularly critical:

a. geostrophic wind analysis

b. surface wind calculation

c. measurement of fetch parameters.

3. Energy transformation processes. Processes or conditions which are believed to affect ocean swell wave energy and are not accounted for in the forecast are the following:

a. cross-sea interference

b. cross or opposing wind

c. viscosity effects.

4. Refraction and shoaling effects.

6C The Energy Forecast

Figure 14 compares the forecast value of E with the observed at site I at the sea surface for the verification times t_1 through t_9. It is noted that the forecast E value lies above the 90% confidence limits of the observed E value at the times t_1,[1] t_4, t_5, and t_8. The inference might be drawn that at these times energy loss processes, not considered in the forecast, are of importance. It is believed significant that a well defined

[1]Additional computations of these data indicate that the correct value of E is approximately identical with the forecast value.

area of cross-sea was present at such location and times as to have interfered with the "swell" arriving at the times t_3, t_4, and t_5 from fetches A and B (Appendix III). Cross-seas are believed to cause the summation of the spectral components to become non-linear giving rise to the conversion of wave energy to turbulent energy by formation of white-caps. Figure 18 illustrates the location and orientation of the cross-sea relative to the generating fetches and the forecast sites at Davenport. Figure 19 displays the spectrum forecast for the cross-sea generating area at six hour intervals over the period when it is most clearly defined. For reasons previously stated, computed spectra for the verification times under discussion, are not available. It is believed that such spectra would have aided greatly in the determination of the portion of the spectrum affected by the cross-sea interference. However, it was noted that if the forecast swell energy were totally erased in the frequency band of the cross-seas, energy reductions of the order of those observed in Figure 14 would have occurred.

Figure 15 compares the forecast values of E with the observed values at site II, at a depth of 80 feet, for the times t_3 through t_9.

By comparing the energy differences which occur at the surface (Figure 14) with the energy differences which occur at depth (Figure 15) it appears it might be permissible to draw inferences about the frequency ranges in which these differences occur. These inferences are based on the fact that the middle and lower frequency energy would be less attenuated with depth by the hydro-dynamic filter than would the high frequency energy. Accordingly, if the relative error of the energy differences at the surface was of the same order as the relative error at depth, it might be inferred that the energy differences were primarily in the

middle and low frequencies. By similar reasoning, if the relative error at depth was significantly less than the relative error at the surface, it might be inferred that the energy differences were primarily in the high frequency end of the spectrum. If the relative error at depth is greater than the relative error at the sea surface the possible causes are less obvious. A possible explanation might be that too much middle or low frequency energy and too little high frequency energy is forecast, the errors cancelling and giving close agreement with the observed energy at the surface. Then, as the forecast spectrum is reduced by the hydrodynamic filter, at depth the surplus middle and low frequency energy which was forecast would be relatively less attenuated with depth than the high frequency energy. Then at depth, the forecast energy by virtue of the surplus middle frequency energy would show a greater relative error than at the surface.

It should be noted that it is quite possible that minor wind systems such as sea-breeze circulations, may have developed between the six hour map intervals of this study which could have developed energy sources not taken into account. Further, because site II is some distance seaward of site I, the total energy at site II is greater as the shoaling effect[1] is less pronounced. Since, in the above discussion, the energy differences are compared between site I at the sea surface and site II at depth, the relative error as observed from Figure 15 will be somewhat greater than would be the relative error at depth at site I.

Examining the relative errors of energy differences at the sea-surface and at depth for the times t_3 through t_9, and applying the

[1] Refraction differences between site I and site II were assumed negligible.

reasoning suggested above, the following comments are offered:

1. At the times t_3 and t_5 the relative erros at the sea-surface and at depth are about the same. At the time t_4 the relative error is much less at depth than at the surface. Following the reasoning suggested above it might be inferred that at times t_3 and t_5 important energy differences occurred in the middle frequencies and that at time t_4 the energy difference was primarily in the high frequency range. As noted previously, it is believed that cross-sea interference acted on the "swell" arriving at these times. These comparisons give rise to the possible conclusion that the forecast spectrum overpredicts in the low and middle frequencies and underpredicts in the high frequencies.

2. At the times t_6 and t_7, the relative error of the energy differences was significantly greater at depth than at the surface. As suggested above, a possible explanation for this may be an overforecast of energy in the middle and low frequencies and an underforecast of energy in the high frequency band. It may be noted that these times are at or near an energy peak. It might be suggested than that for higher wind speeds the assumed energy spectrum overpredicts in the middle frequencies and underpredicts in the higher frequencies. At least such an assumption is consistent with these data.

3. At the times t_8 and t_9 the relative error at the surface is significantly larger algebraically than at depth. Following the line of reasoning used for time t_4, it might be inferred that important energy differences occurred in the high frequency band. The cause of this assumed high frequency energy reduction is not readily apparent. It is noted, however, that at both time t_4 and t_8 the observed energy is at a minimum. A

possible explanation might be that at lower wind speeds the assumed energy spectrum may overpredict in the high frequency end of the spectrum.

6D Summary

In summary, it is the opinion of the authors that the forecast method for swell is operationally useful for fetches of the type active in this study. Based on this investigation, it appears that the curves and procedures of the method [6] , when properly applied, will result in a wave forecast of useful accuracy. Figure 22, a plot of the forecast significant wave height compared to the observed illustrates this conclusion. As noted in paragraph 6A above, the results are consistent with the assumption that energy reduction processes not considered in the forecast are at times important. In particular, it is believed that cross-sea interference was responsible for significant energy reductions at certain verification times in this investigation. It is believed that a qualitative correction would be possible by reducing the forecast spectrum by a fraction of the cross-sea spectrum developed.

The data are also consistent with the premise that, for increasing wind speeds, the forecast energy spectrum is too high in the low and middle frequencies and possibly too low in the high frequency band, and that for lower wind speeds, an opposite trend appears possible.

6E Future Research

When certain modifications in the computer programs discussed in Chapter 4 are completed, and accurate observational spectra are available, more definite conclusions will be possible. It is believed that cross-sea effects may become quite clear from a comparison of the forecast and the observed spectra. It is the opinion of the authors that extensions of the

methods used in this investigation can provide the quality and quantity of data necessary for the evaluation of forecast methods and the effects of attenuation.

FIGURE 1

CONTINOUS WAVE SPECTRUM FOR FULLY ARISEN SEA

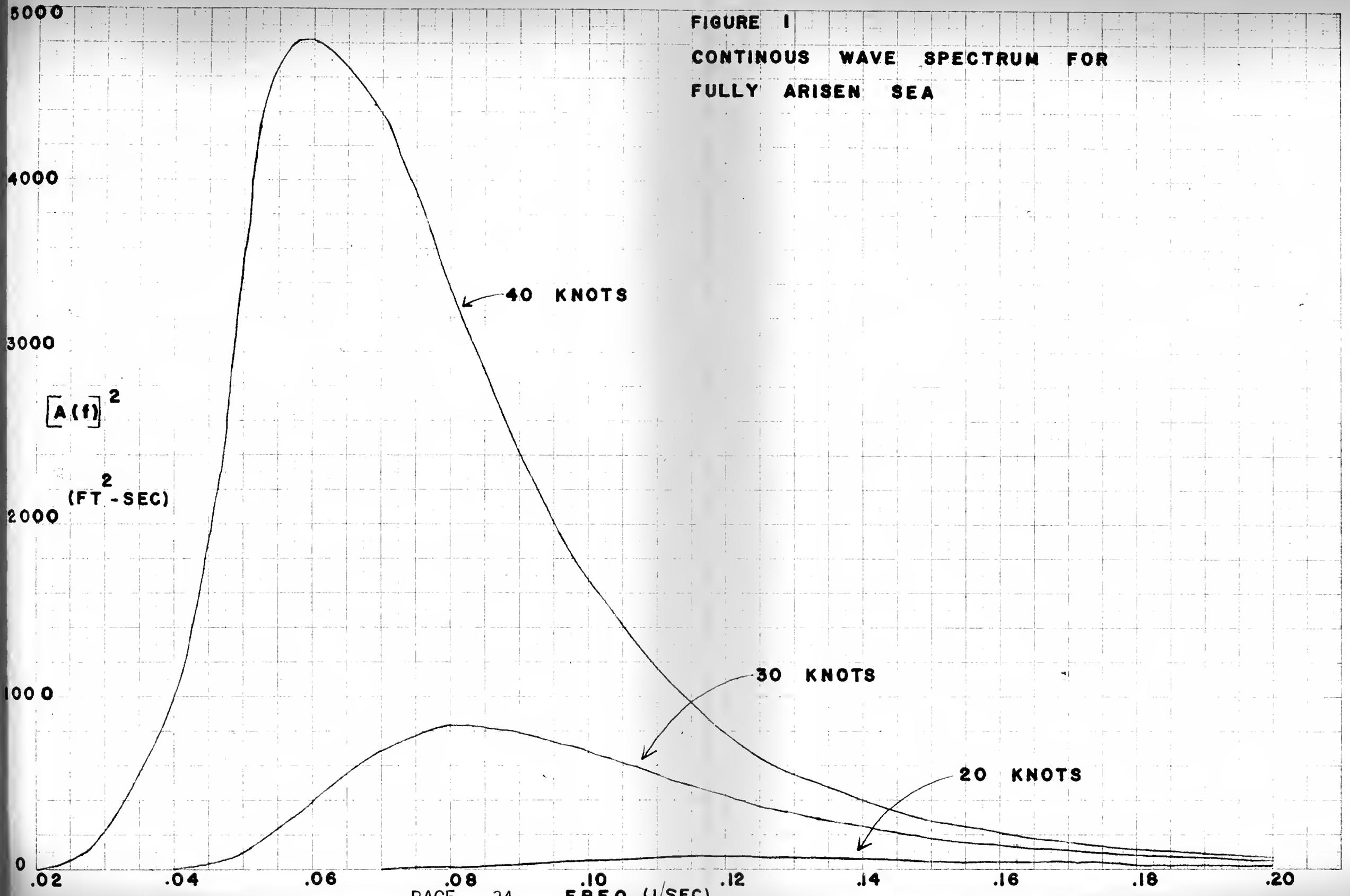

FIGURE 2 WAVE SPECTRUM AND CO-CUMULATIVE SPECTRUM

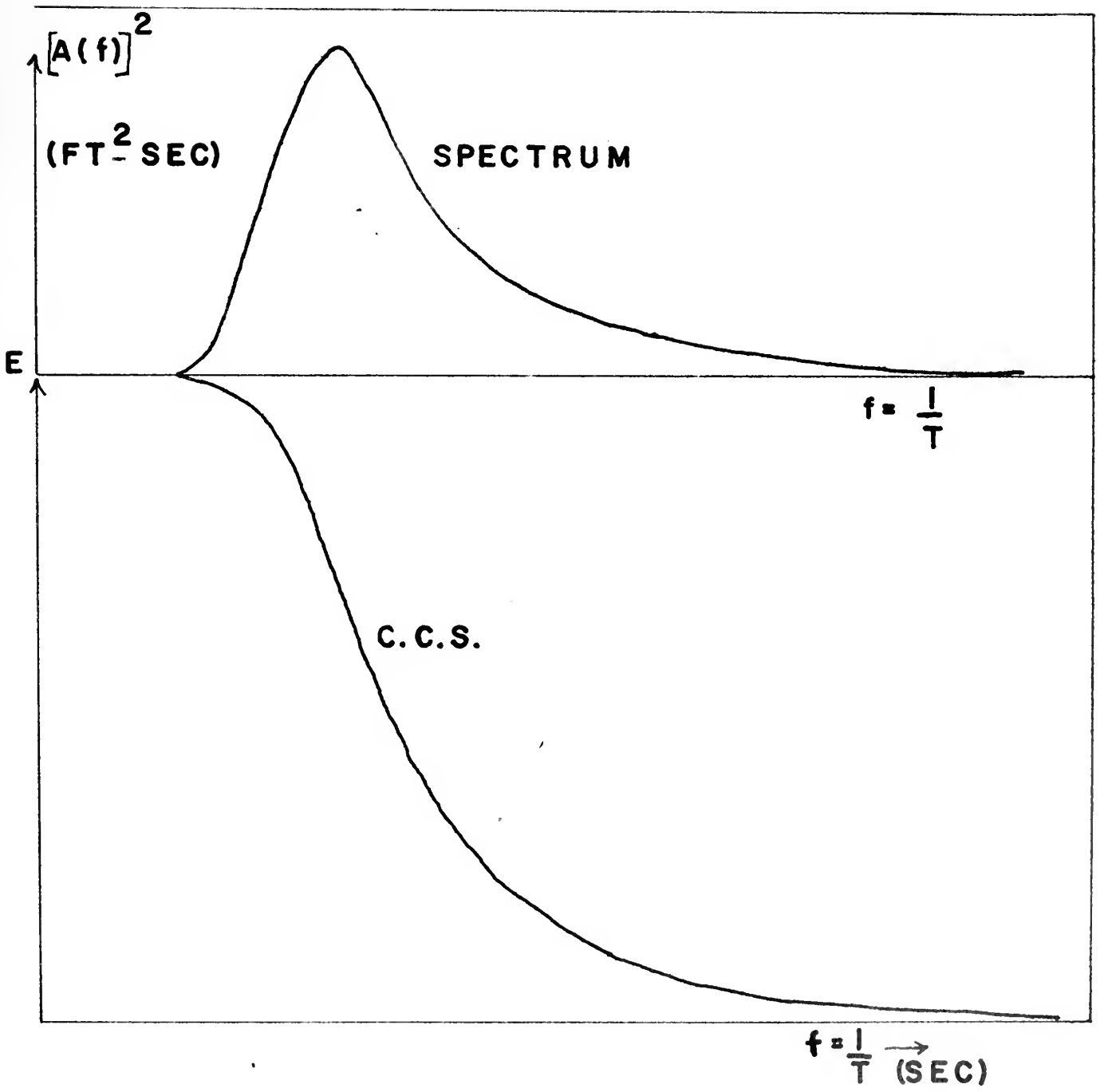

FIG. 2

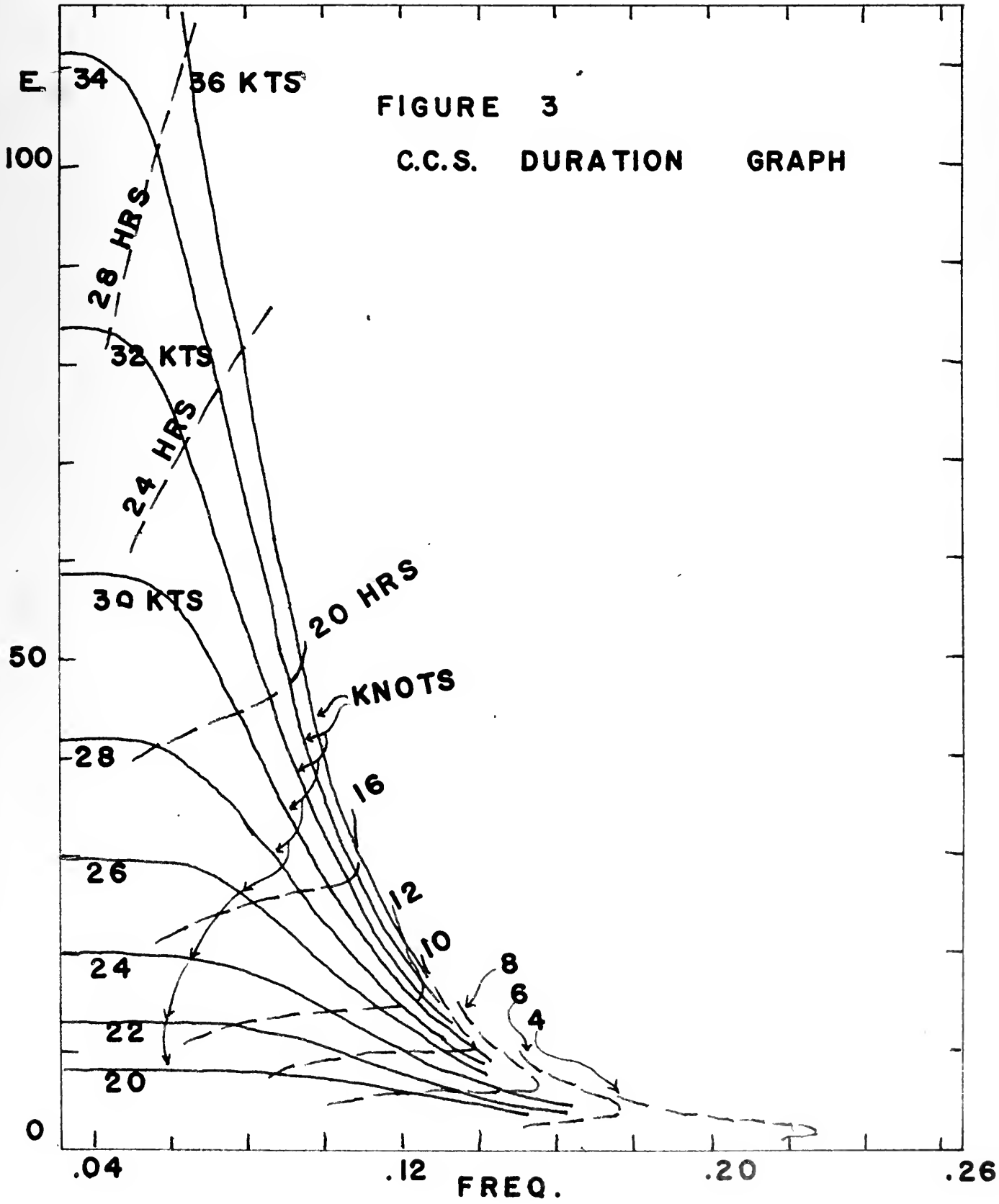
FIGURE 3
C.C.S. DURATION GRAPH
E
100
50
0
34
36 KTS
28 HRS
32 KTS
24 HRS
30 KTS
20 HRS
KNOTS
28
16
26
12
10
24
8
6
4
22
20
.04
.12
.20
.26
FREQ.

FIG. 3

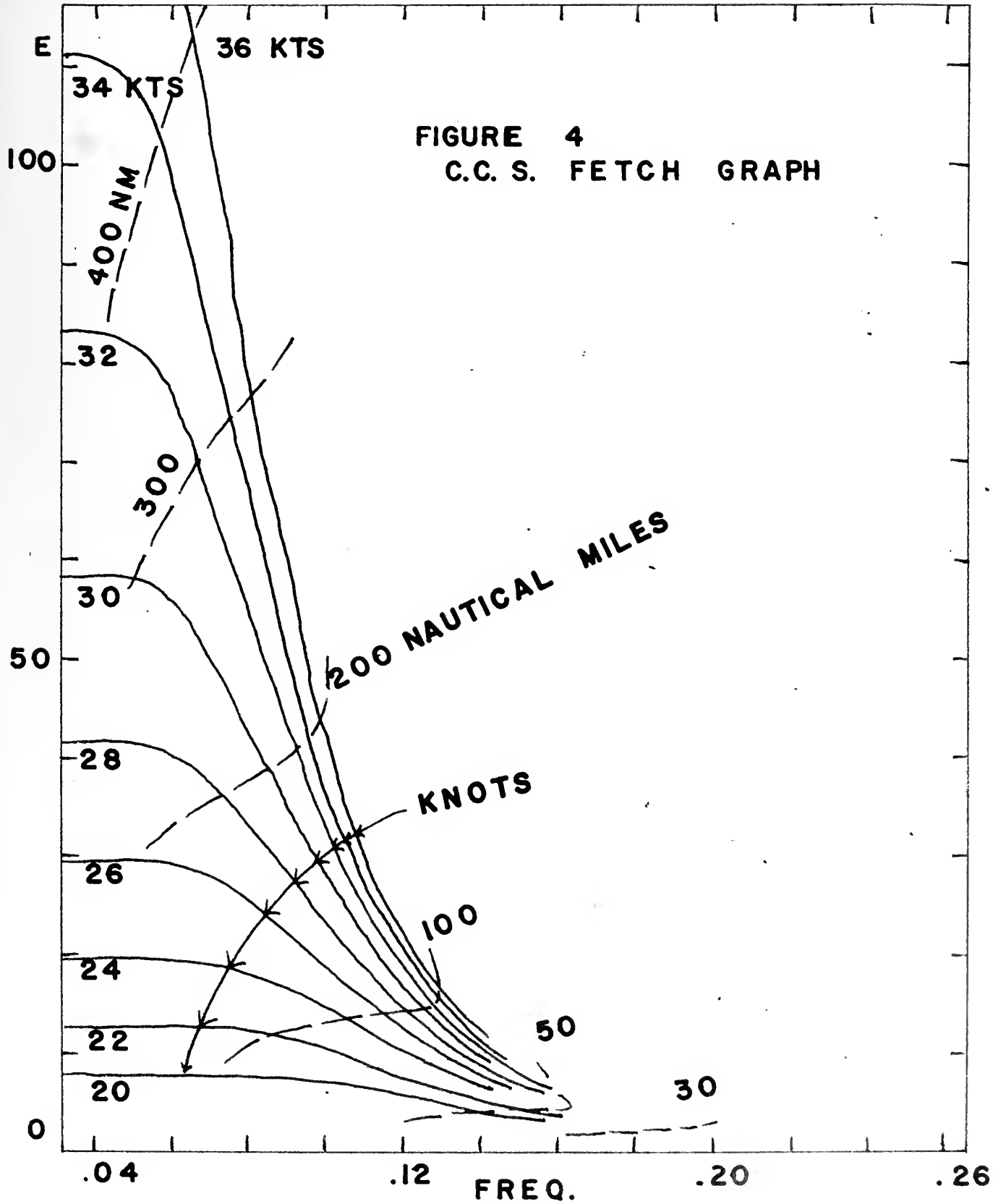

FIGURE 4
C.C. S. FETCH GRAPH

FIG. 4

FIGURE 5

THE EFFECT OF DIRECTIONS IN THE FILTER

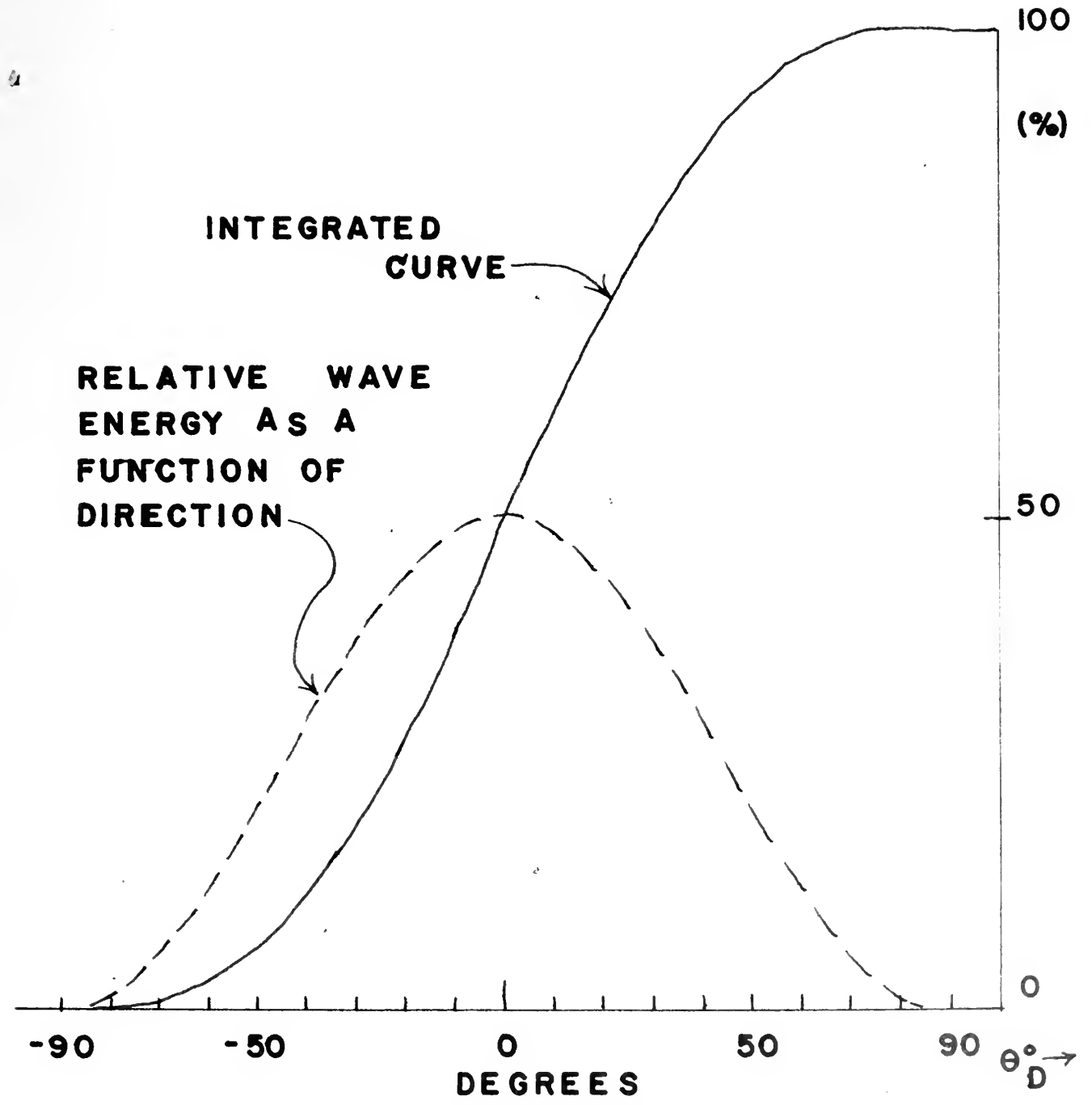

FIG. 5

FIGURE 6

DEFINITION OF θ_3 AND θ_4

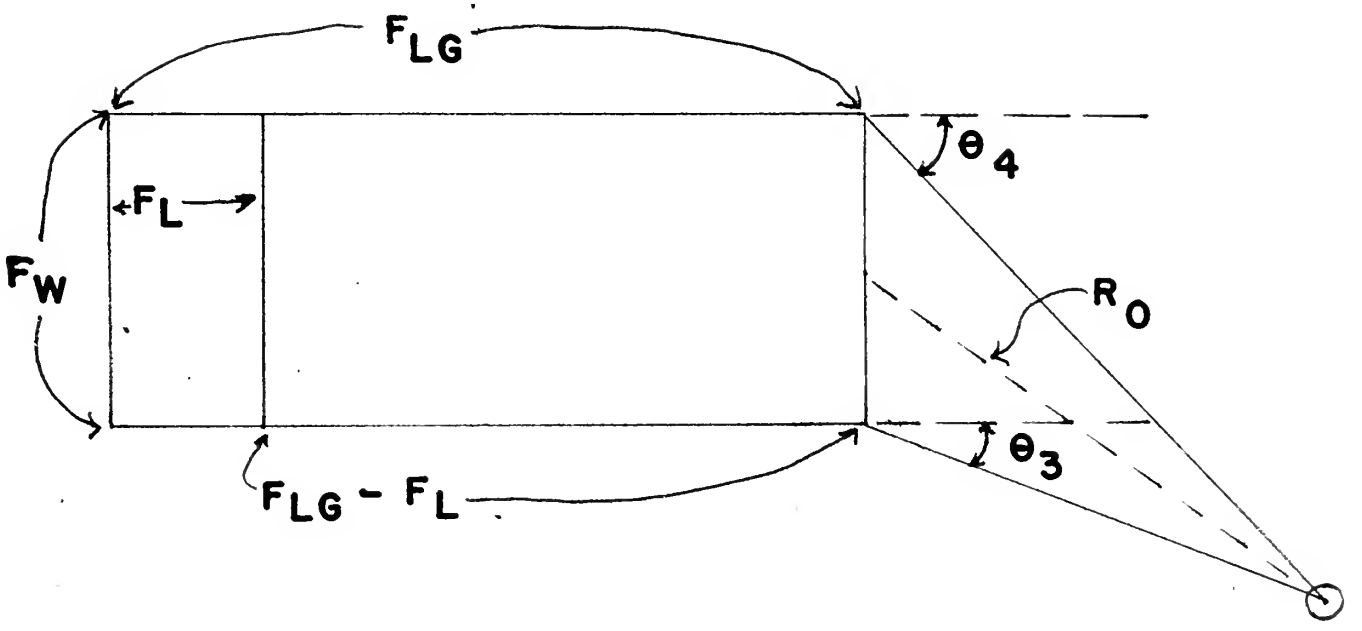

FIG. 6

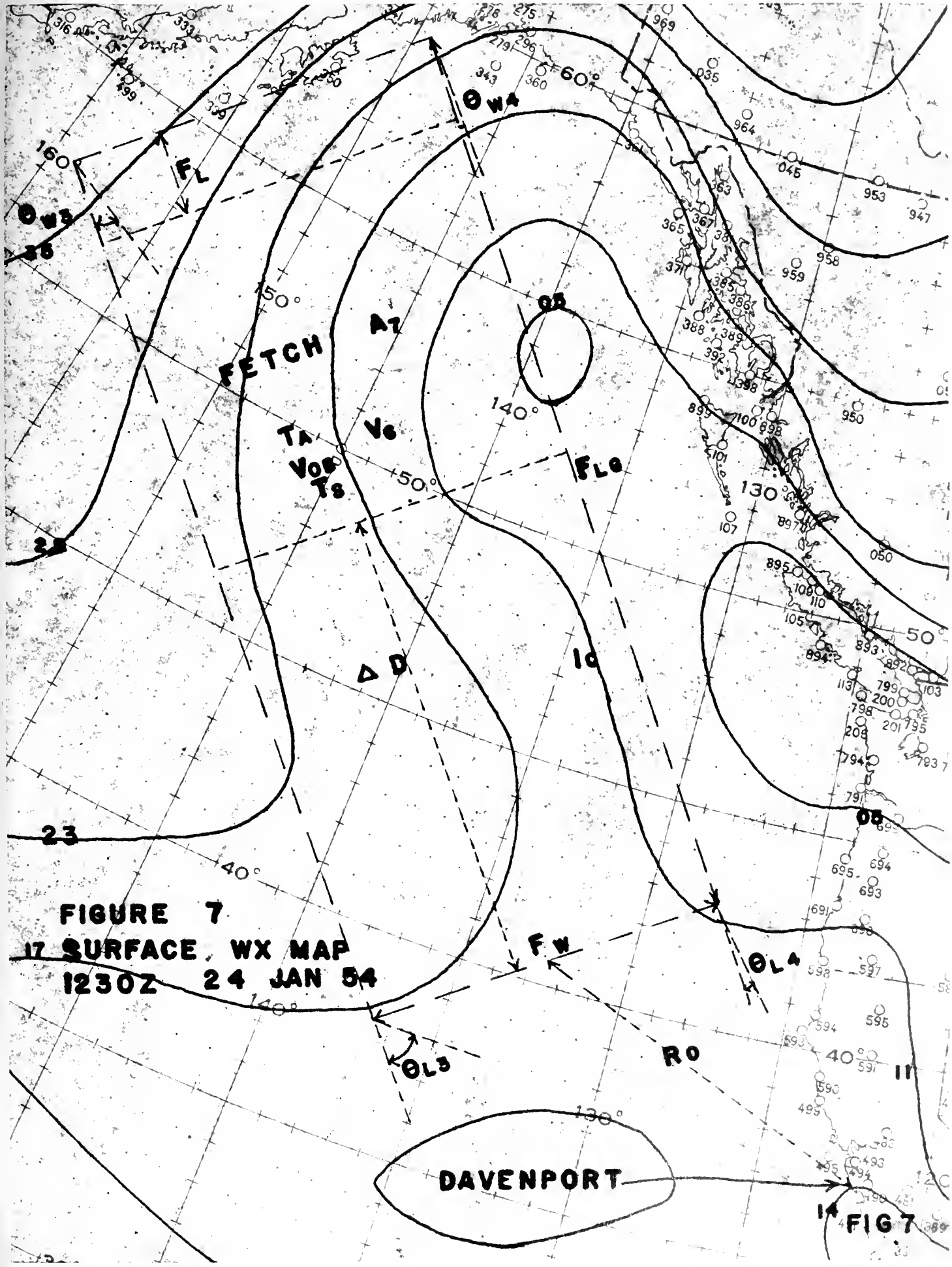

FIGURE 7
17 SURFACE WX MAP
1230Z 24 JAN 54

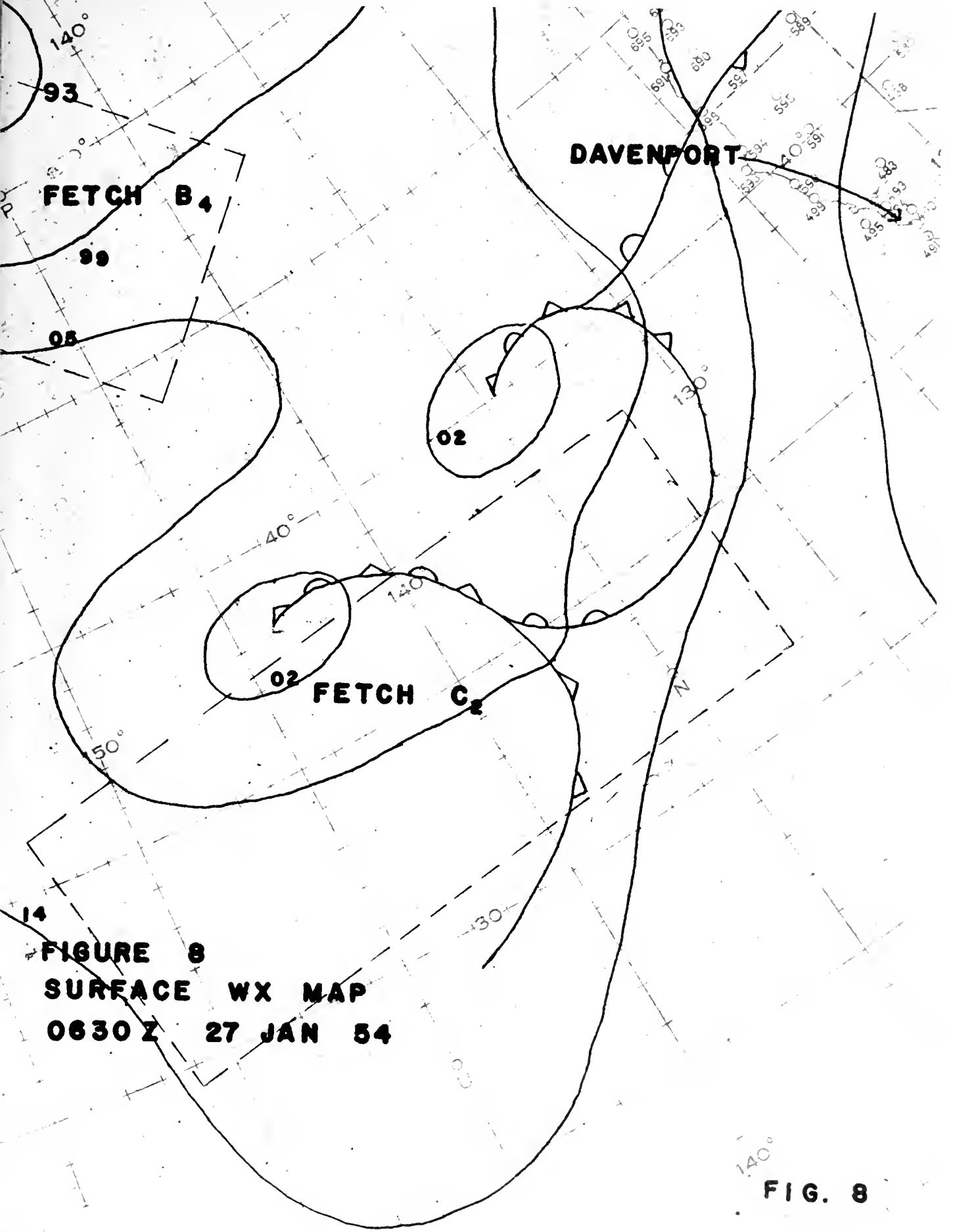

FIGURE 8
SURFACE WX MAP
0630 Z 27 JAN 54

FIG. 8

FIGURE 9A

T_U AND T_L AS A FUNCTION OF TIME

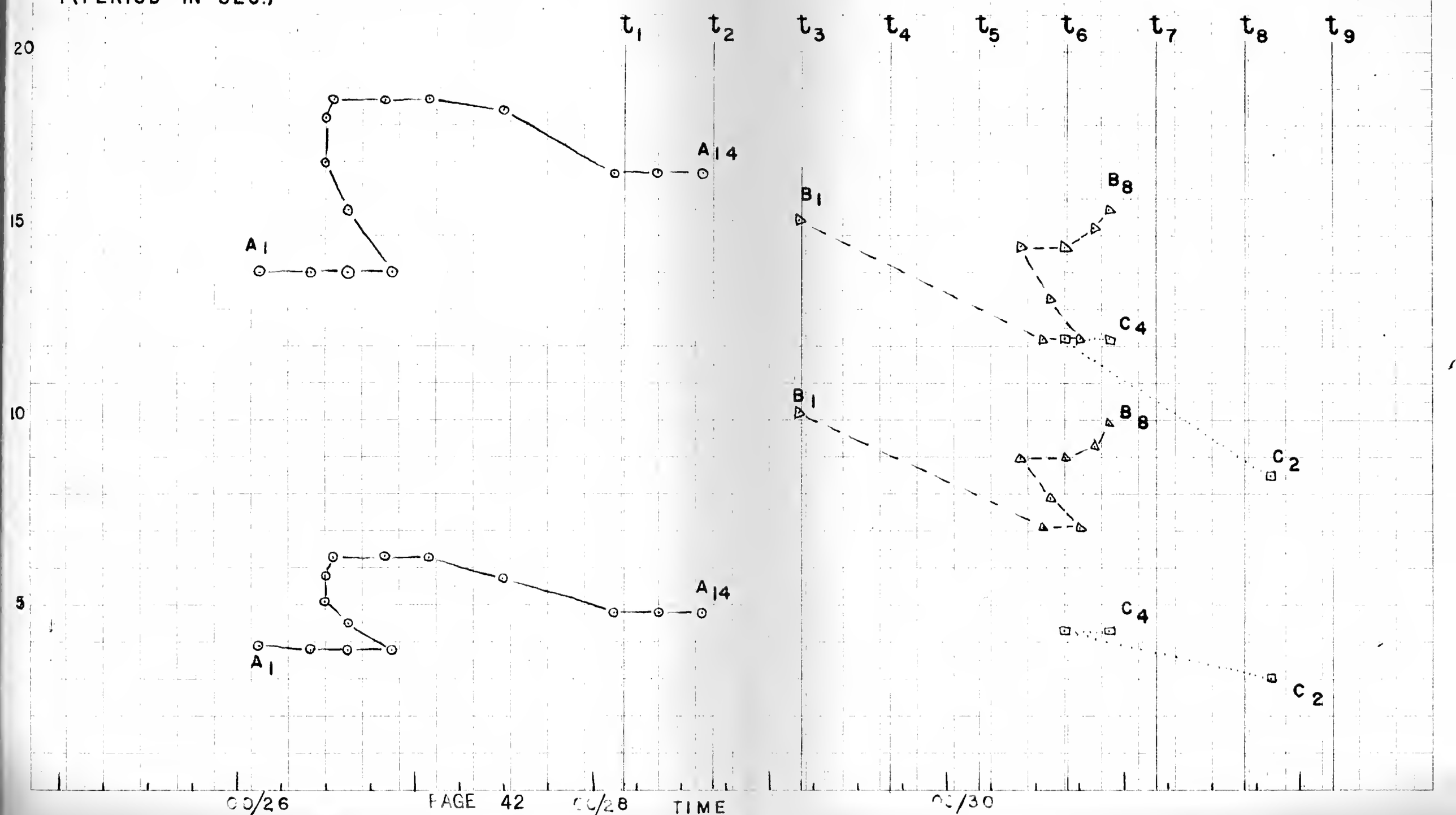

FIGURE 9B DISPERSON ENVELOPE

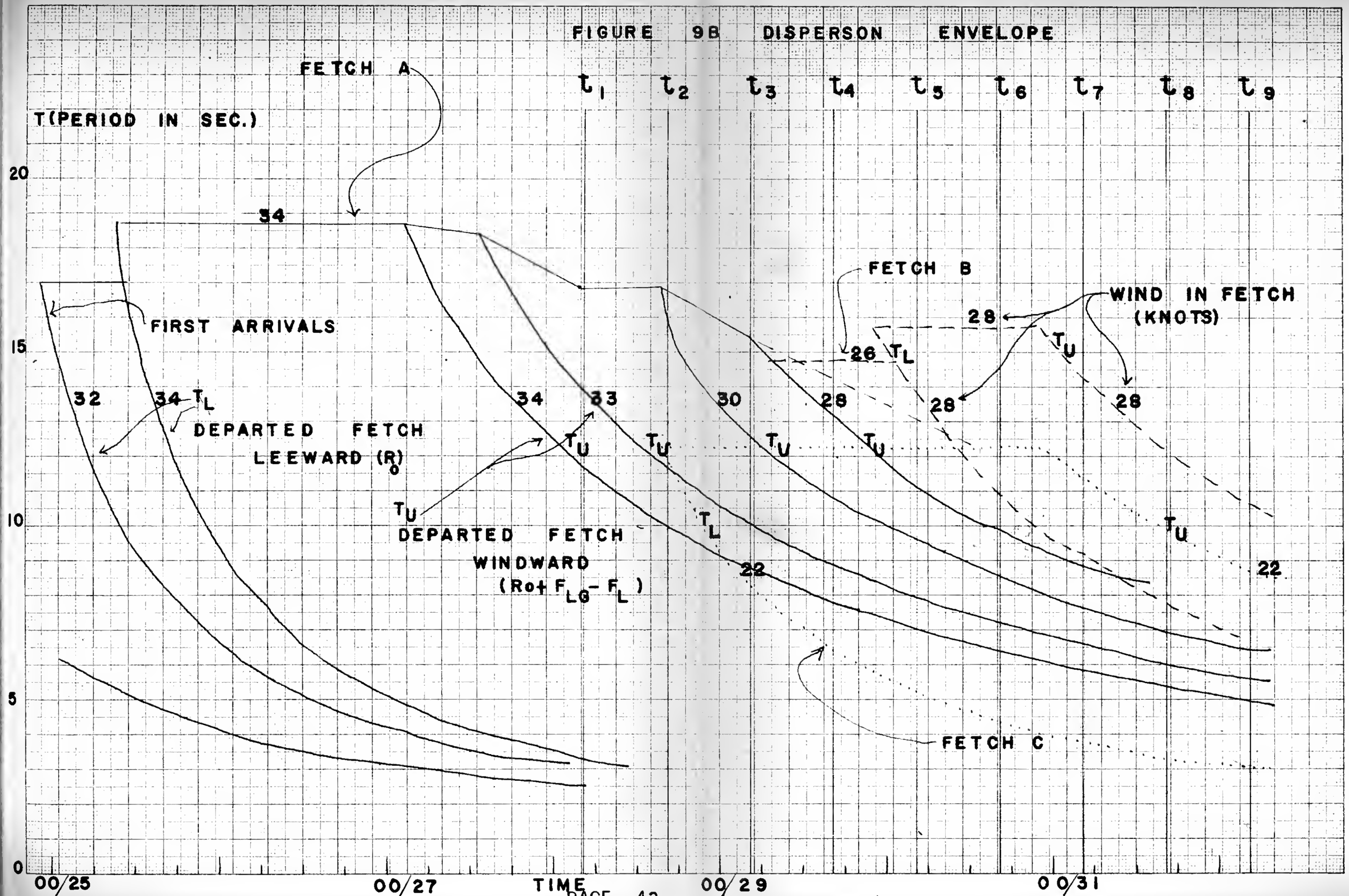

FIGURE 10

FORECAST SPECTRAL ENERGY
PRESENT AT DAVENPORT, CALIF.
AT t_1

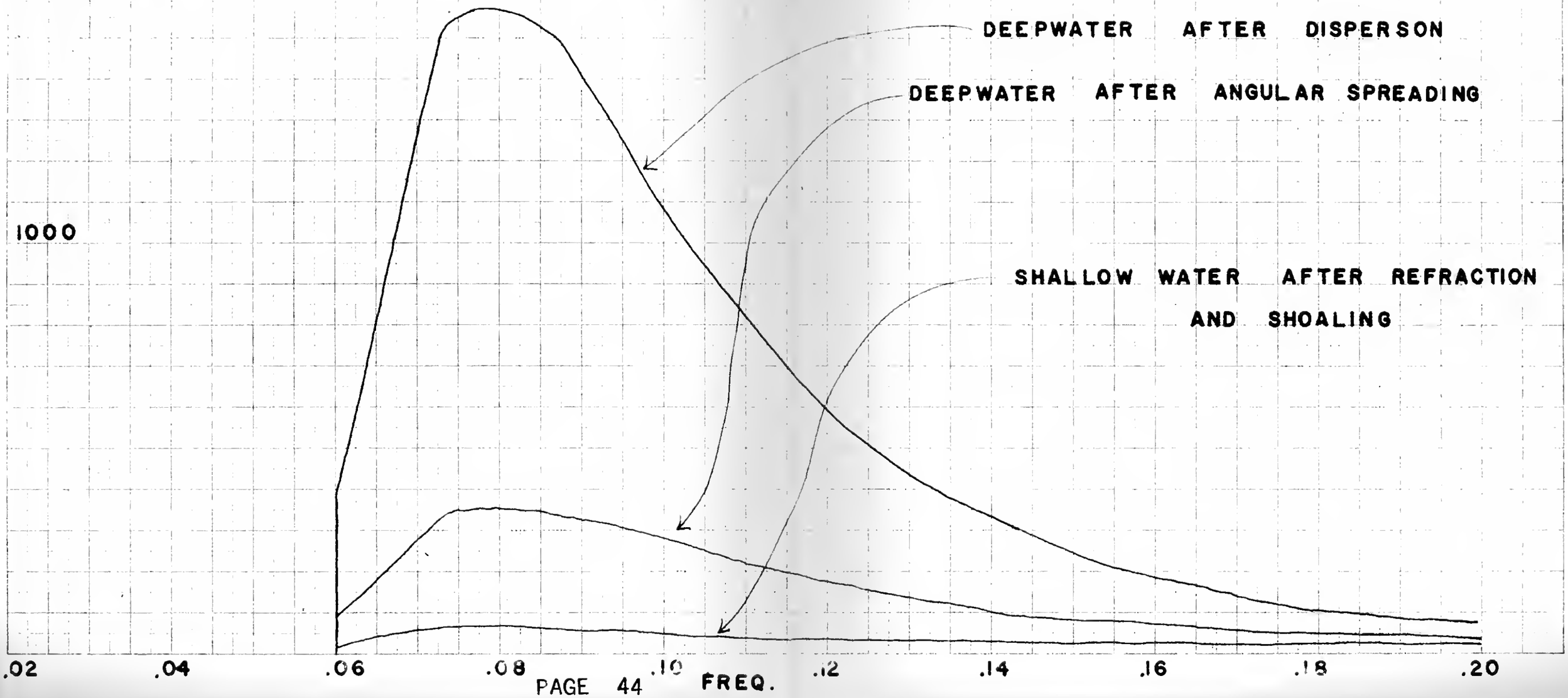

FIGURE II

FORECAST SPECTRAL ENERGY PRESENT AT DAVENPORT AT t_4 (COMPOSITE FROM A, B, AND C)

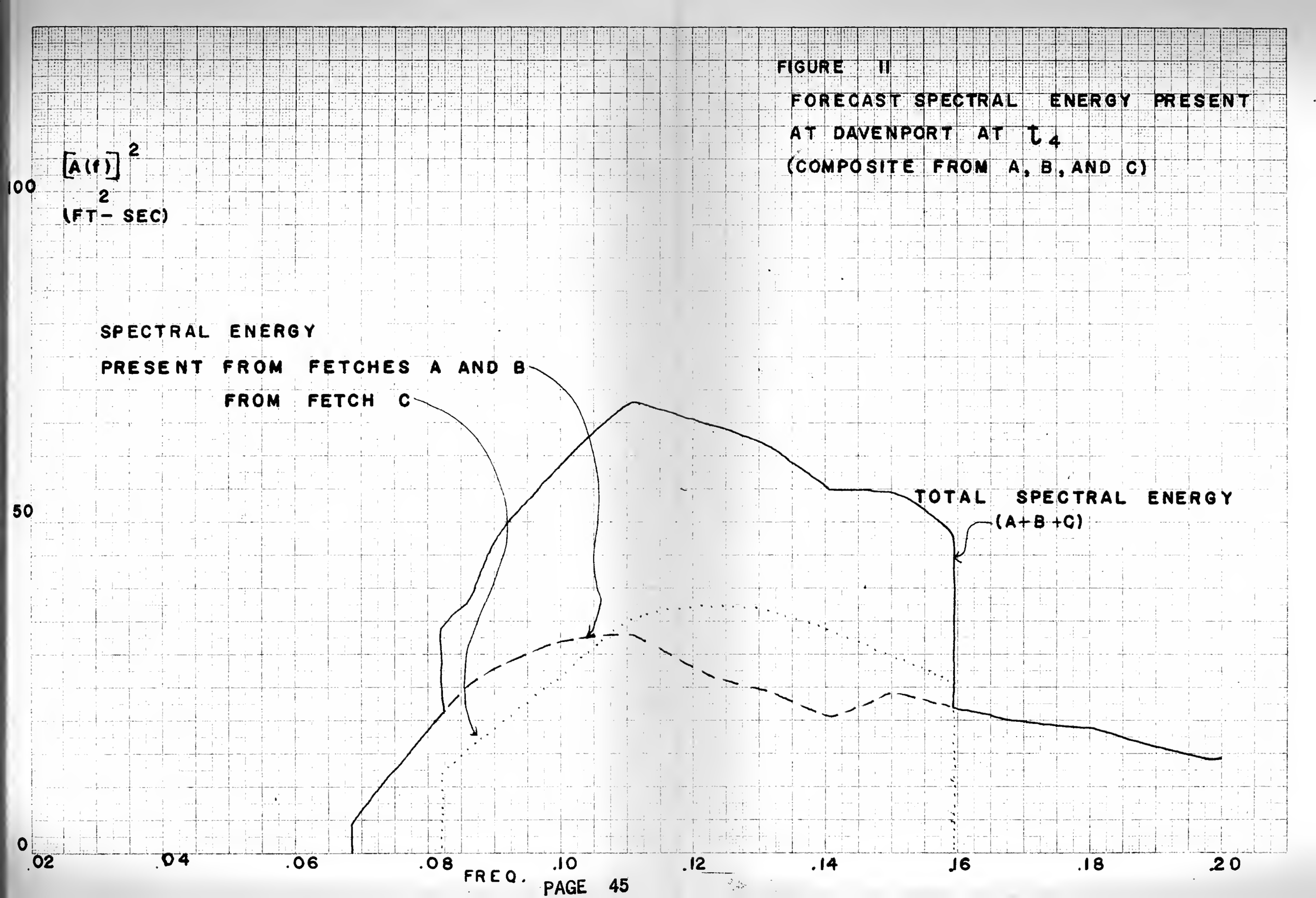

FIGURE 12

VARIATIONS OF THE ANGULAR SPREADING FACTOR IN DIFFERENT PORTIONS OF THE FETCH

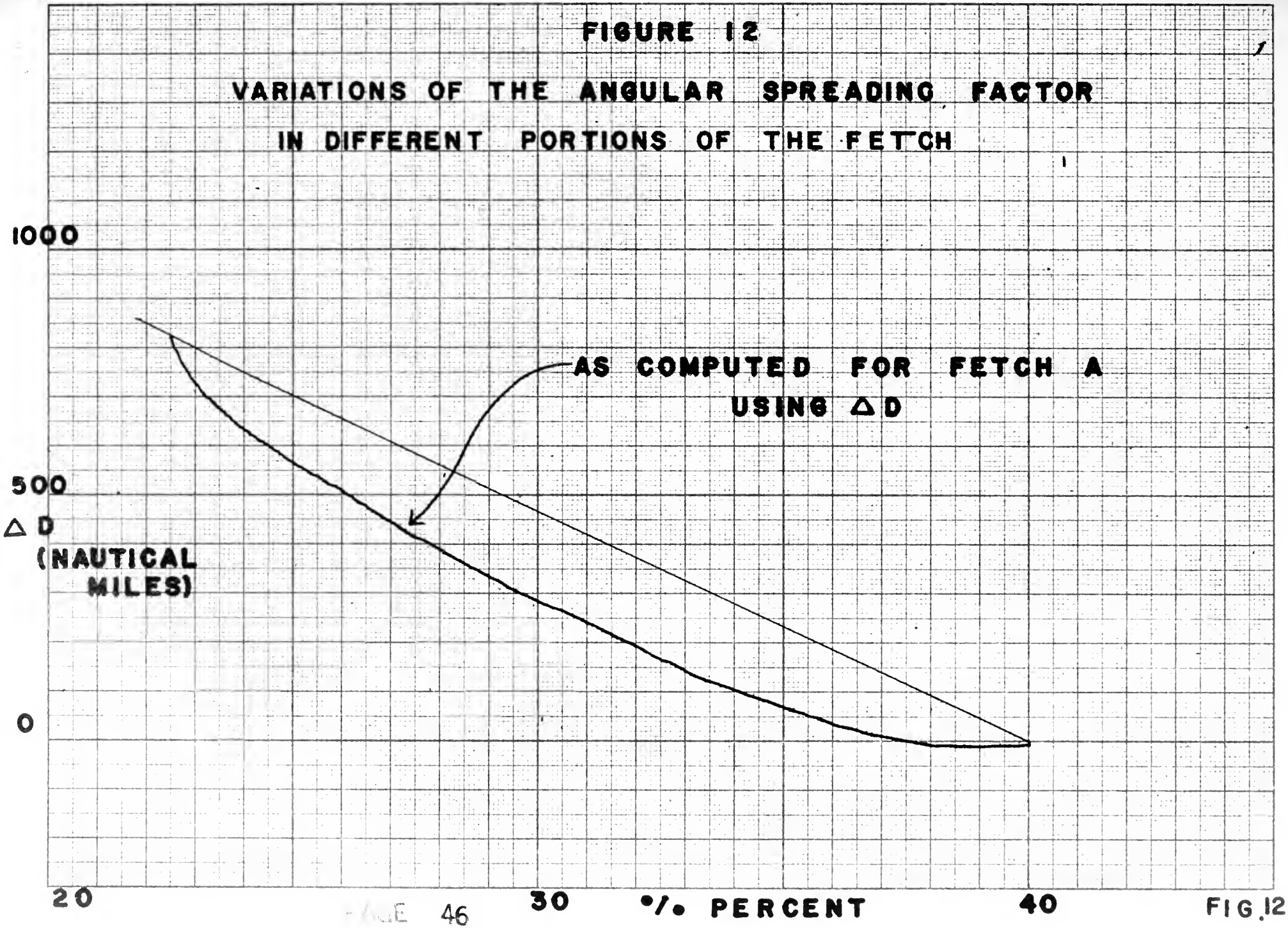

FIG. 12

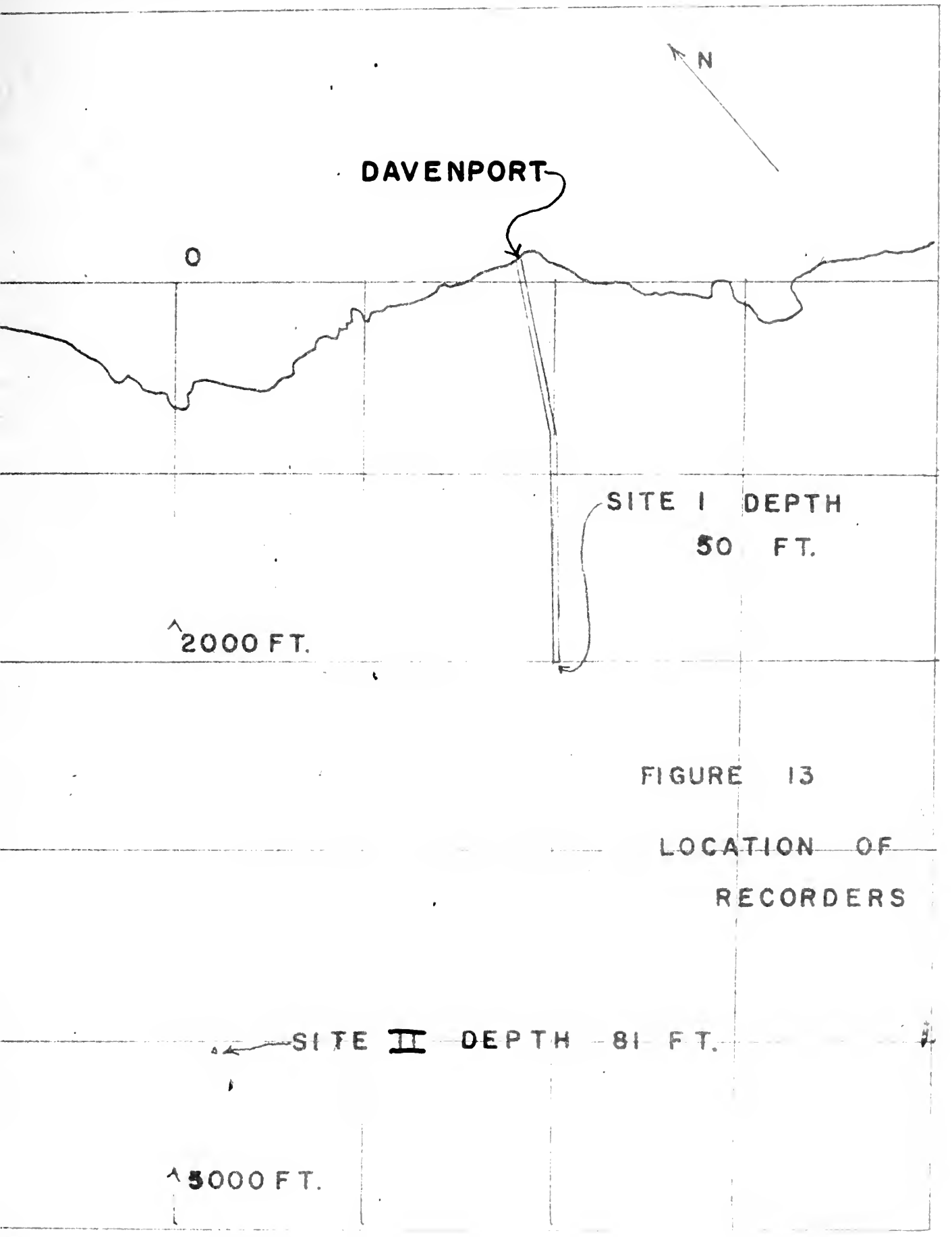

FIGURE 13

LOCATION OF
RECORDERS

FIGURE 14

COMPARISON OF E AT DAVENPORT, CALIF.
(AT SURFACE -- WATER DEPTH 50 FT.)

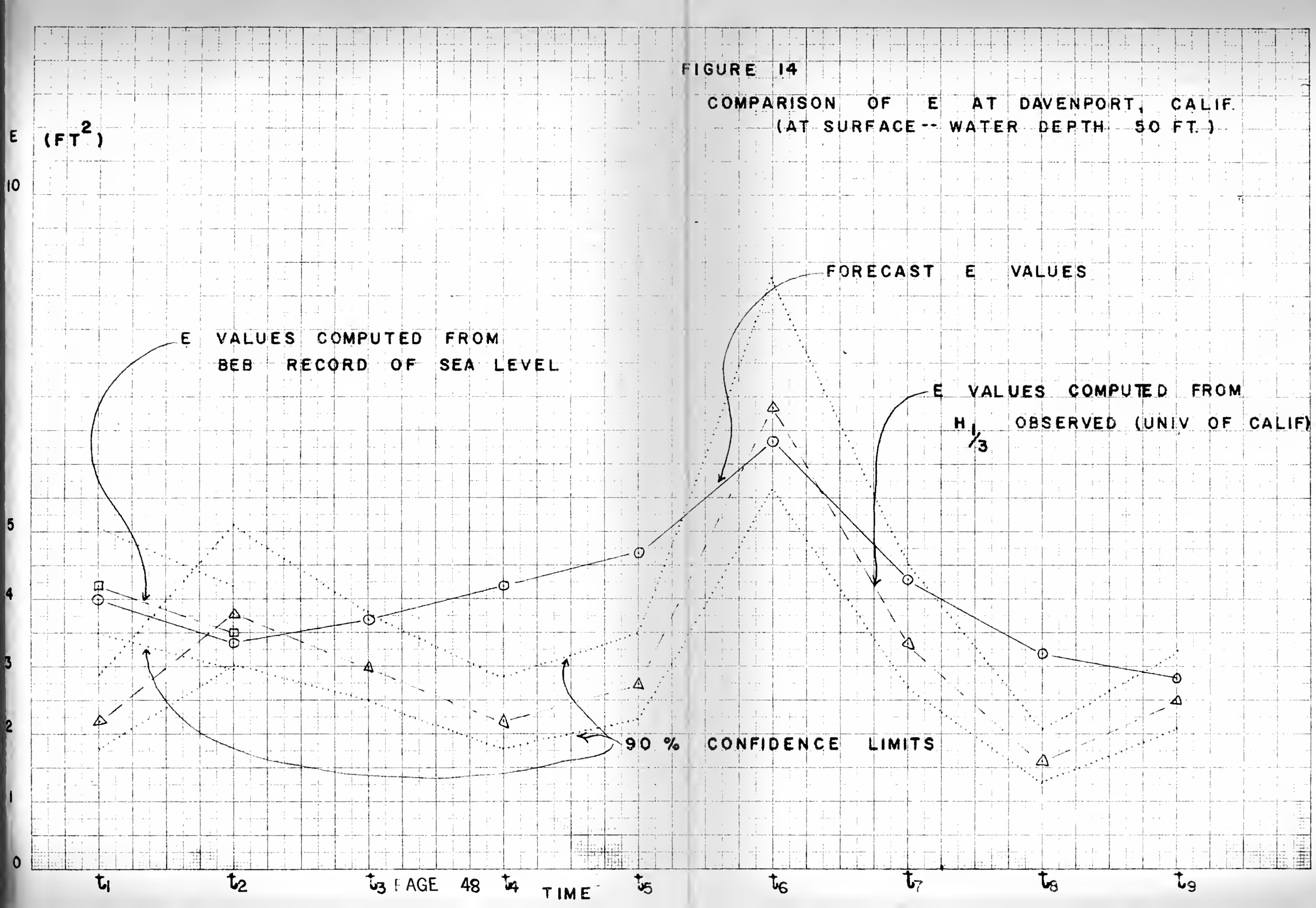

FIGURE 14

COMPARISON OF E AT DAVENPORT, CALIF.
(AT SURFACE -- WATER DEPTH 50 FT.)

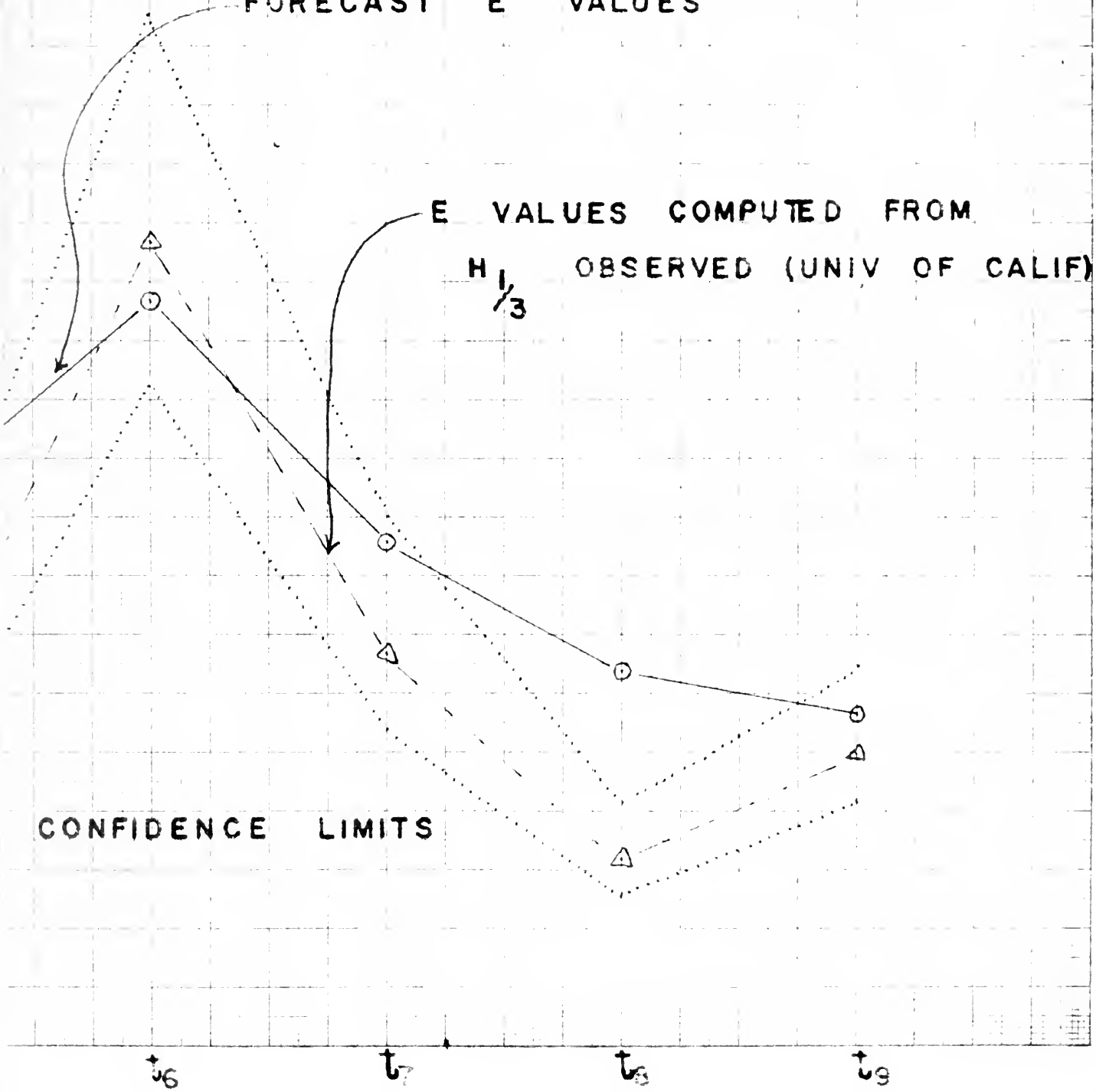

FIGURE 15

COMPARISON OF E AT DAVENPORT

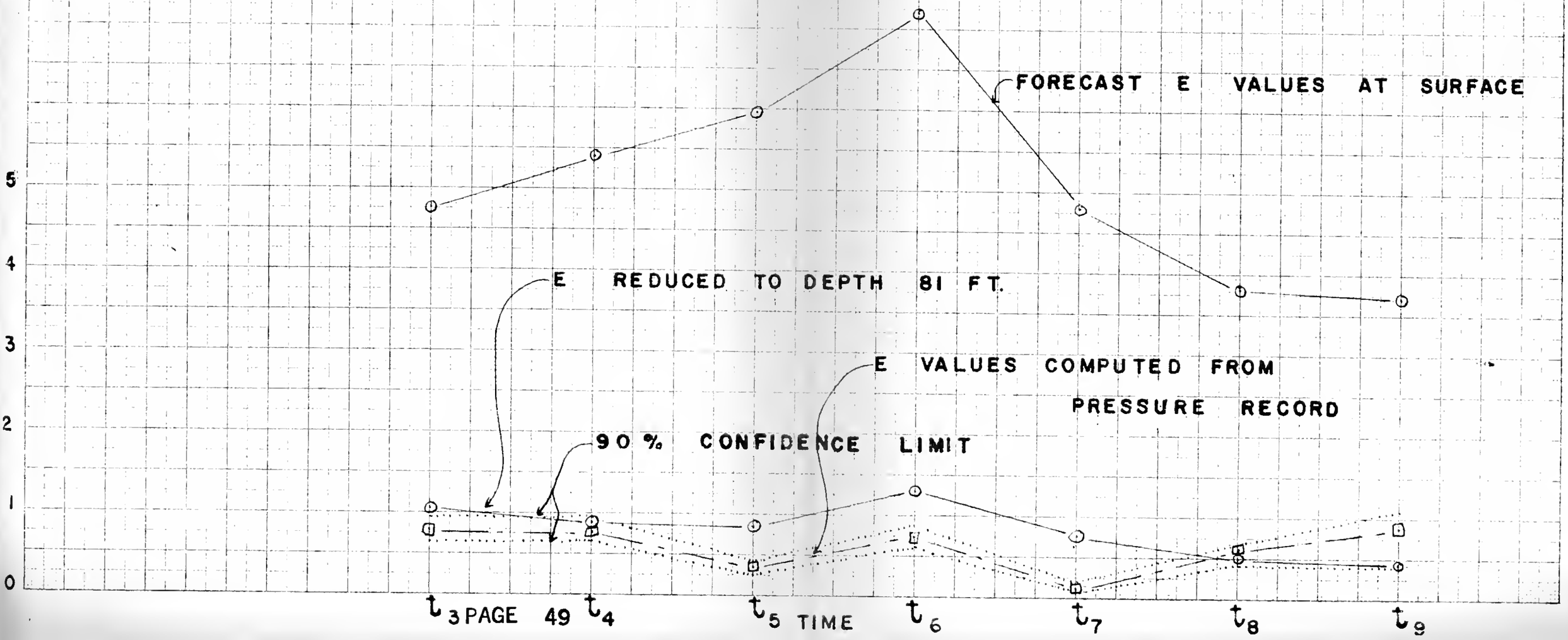

FIGURE 16

COMPARISON TIME T_5

100

$(FT^2\text{-SEC})$

$[A(f)]^2$

FORECAST SPECTRAL ENERGY AT SEA SURFACE

AT DEPTH OF 81 FEET

50

0

.02 .04 .06 .08 .10 .12 .14 .16 .18 .20

FREQ.

FIGURE 17

COMPARISON TIME t_7

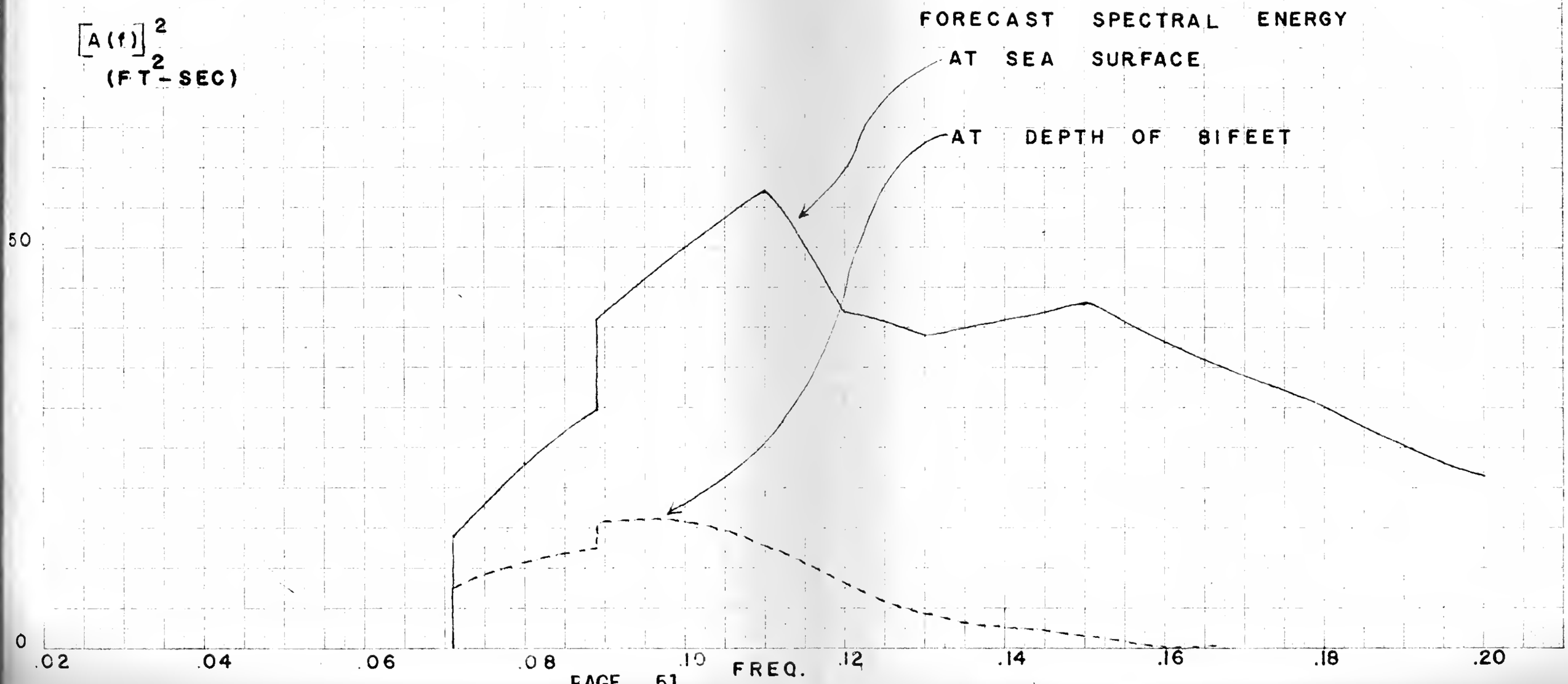

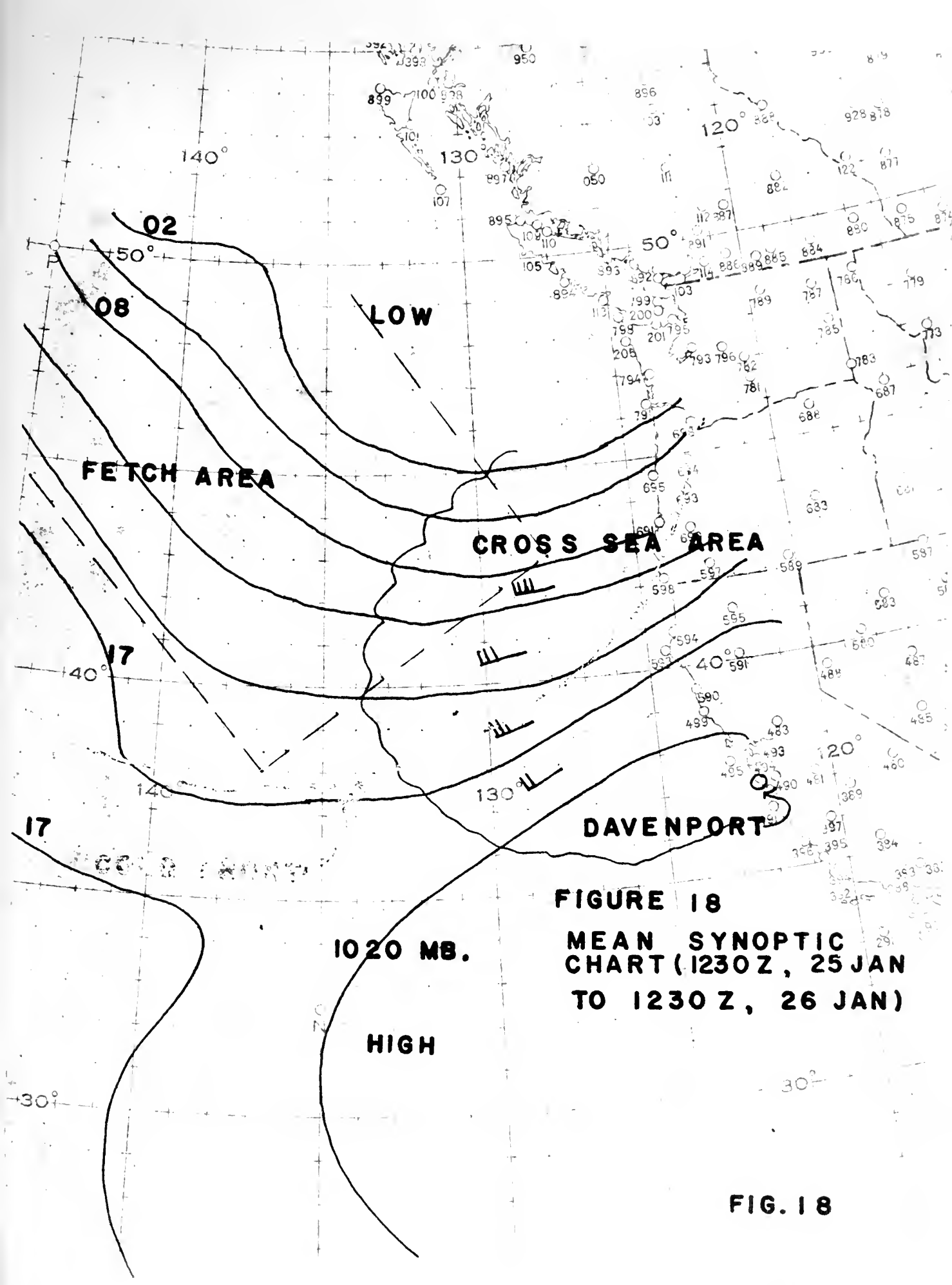

FIGURE 18

MEAN SYNOPTIC CHART (1230Z, 25 JAN TO 1230Z, 26 JAN)

FIG. 18

FIGURE 19

SPECTRUM OF CROSS SEA

AT TIME 1830 Z 25 JAN

0030 Z 26 JAN

0630Z 26 JAN

$[A'(f)]^2$

150 $(FT^2 - SEC)$

100

50

0

.02 .04 .06 .08 .12 .14 .16 .18 .20

FREQ.

0030Z/26

0630Z/26

1830Z/25

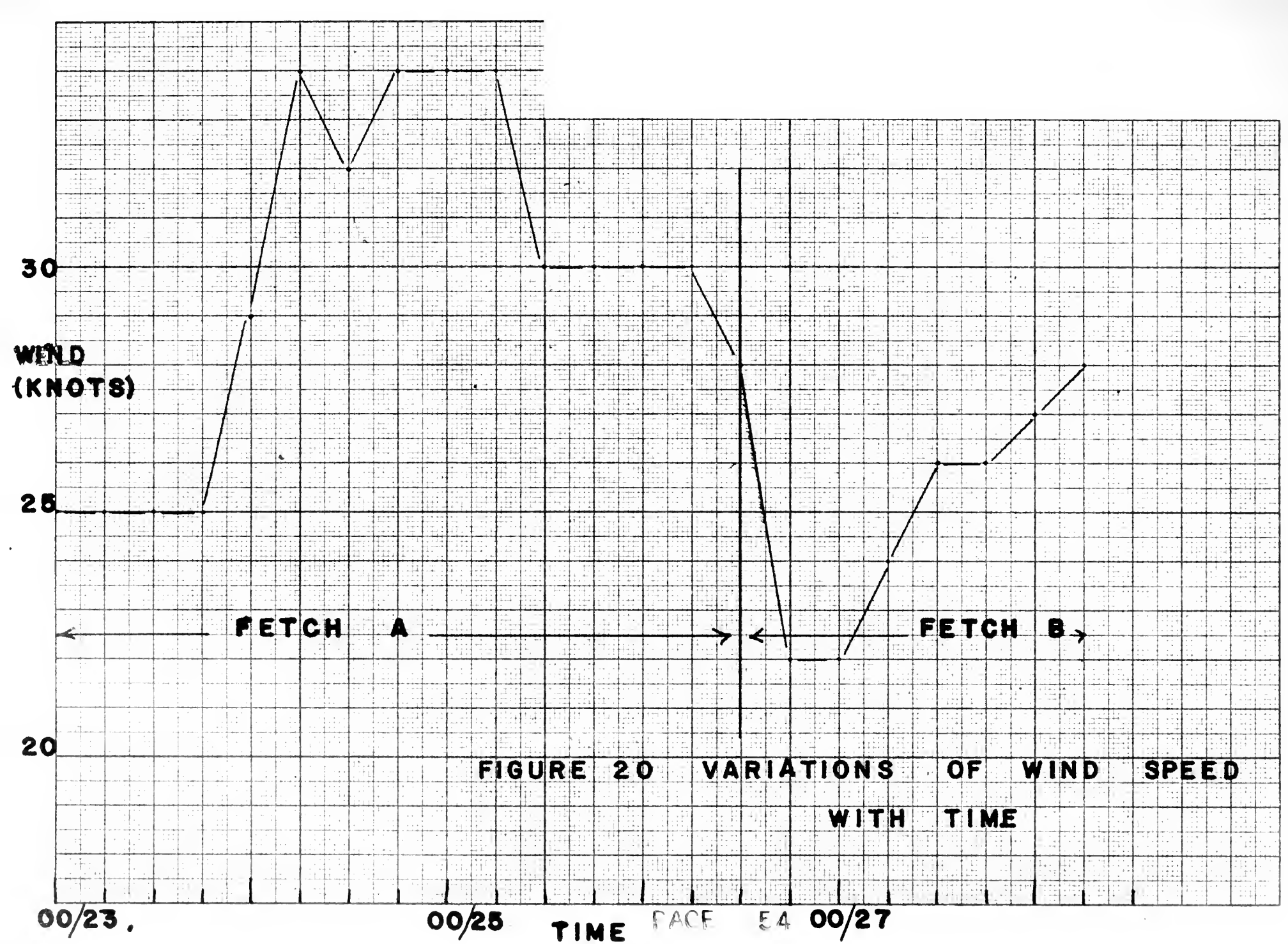

FIGURE 20 VARIATIONS OF WIND SPEED WITH TIME

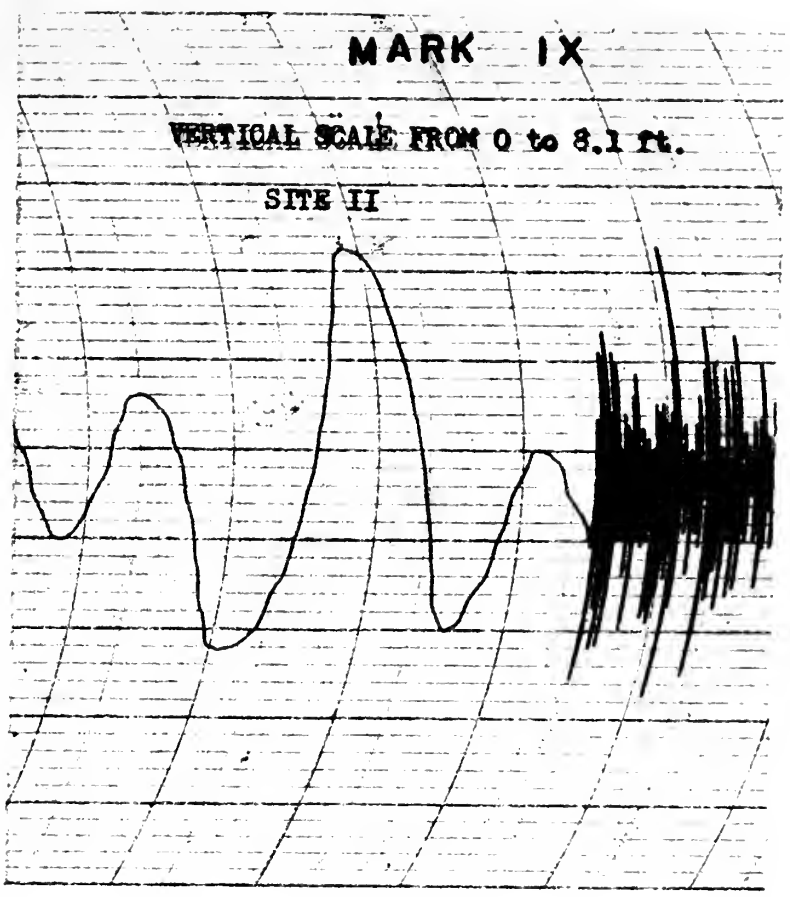

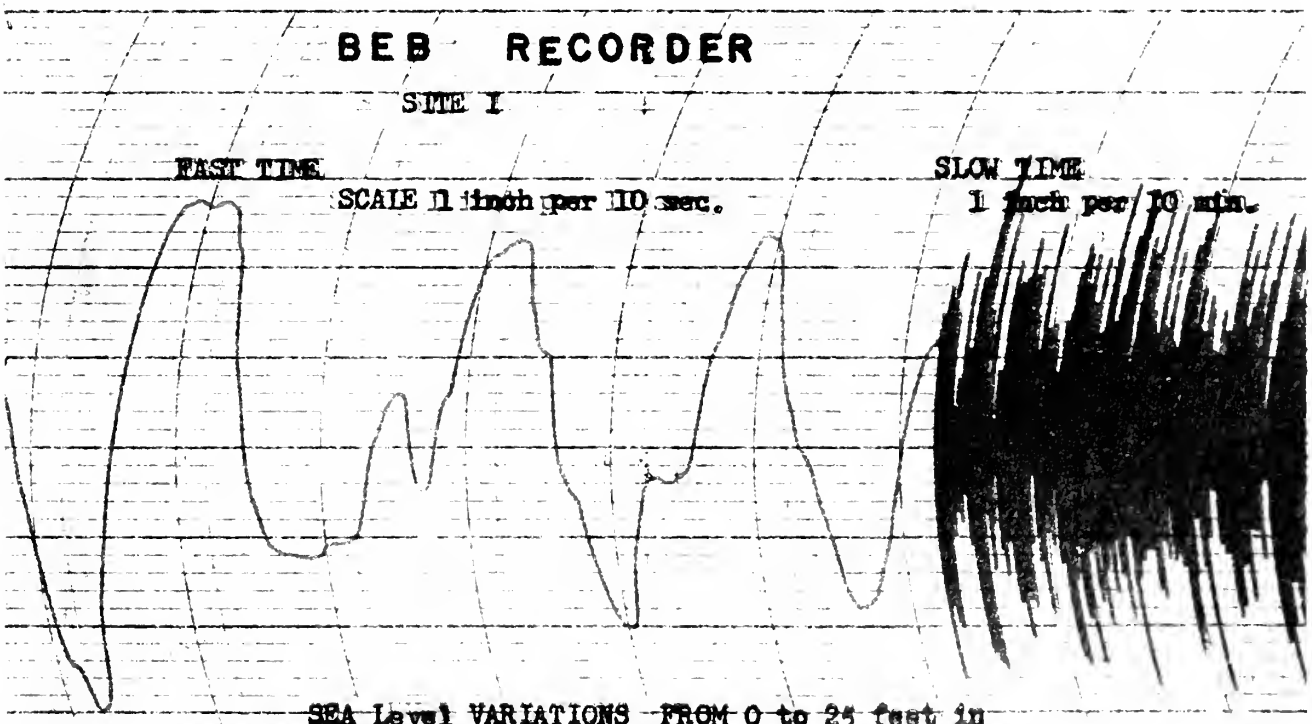

FIGURE 21 ILLUSTRATIONS OF A WAVE RECORD

FIGURE 22

COMPARISON OF SIGNIFICANT WAVE HEIGHTS ($H_{1/3}$) AT SITE I

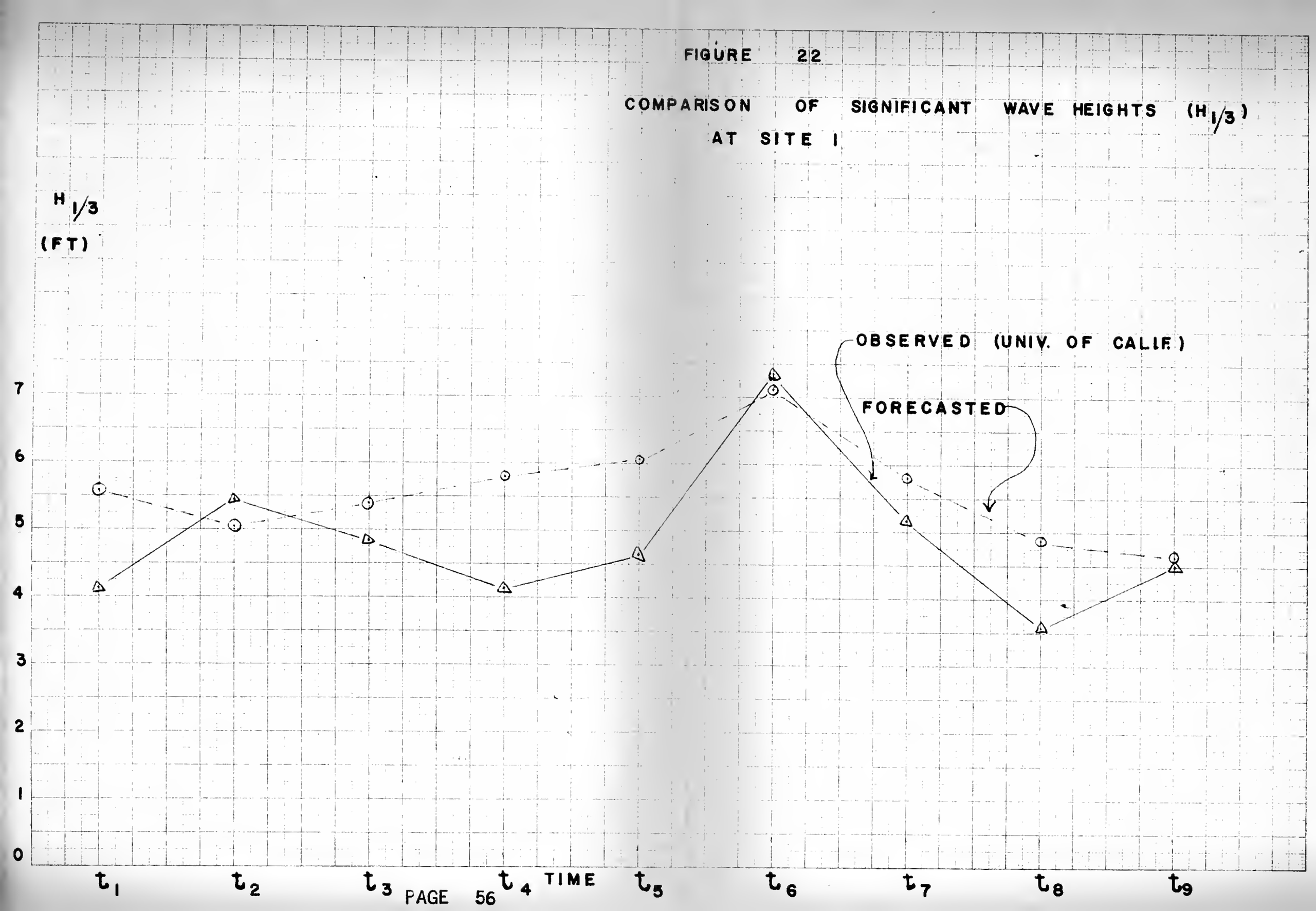

TABLE 1

WAVE HEIGHT DATA AS A FUNCTION OF E

Approximate Wave Height Data 10% Ranges

10%	between	0.00		and	$0.64\sqrt{E}$	ft.
10%	"	0.64	$\sqrt{E}$	"	$0.94\sqrt{E}$	ft.
10%	"	0.94	$\sqrt{E}$	"	$1.20\sqrt{E}$	ft.
10%	"	1.20	$\sqrt{E}$	"	$1.42\sqrt{E}$	ft.
10%	"	1.42	$\sqrt{E}$	"	$1.66\sqrt{E}$	ft.
10%	"	1.66	$\sqrt{E}$	"	$1.92\sqrt{E}$	ft.
10%	"	1.92	$\sqrt{E}$	"	$2.20\sqrt{E}$	ft.
10%	"	2.20	$\sqrt{E}$	"	$2.54\sqrt{E}$	ft.
10%	"	2.54	$\sqrt{E}$	"	$3.04\sqrt{E}$	ft.
10%	greater than	$3.04\sqrt{E}$				

Most frequent Wave Height	$1.41\sqrt{E}$ ft.
Average Height	$1.77\sqrt{E}$ ft.
Significant Height (Average of highest 1/3)	$2.83\sqrt{E}$ ft.
Average of Heights of 1/10 Highest Waves	$3.60\sqrt{E}$ ft.

TABLE 2

DATA OBTAINED FROM SYNOPTIC MAPS

Map Time GCT	Fetch Desig.	Fetch Width F_W	Fetch Length F_{LG}	Observed Winds (Beaufort)[2] V_{ob}	Sea Temp. T_s	Air Temp. T_a	Geostrophic Wind [1] V_g	Isobar Curvature I_c [3]	Distance Fetch to Observ. Pt. R_o
0030 23 Jan	A_1	500	1320	6	41	39	23	S	450
0630	A_2	520	1320	6	41	41	19	S	450
1230	A_3	540	1320	6	40	40	23	S	420
1830	A_4	510	1320	6	40	34	27	C	420
0030 24 Jan	A_5	510	1320	8	41	32	27	C	420
0630	A_6	510	1320	8	41	40	30	C	420
1230	A_7	510	1320	7	42	42	27	S	420
1830	A_8	510	1320	8	41	38	29	S	420
0030 25 Jan	A_9	510	1320	8	41	38	28	C	420
0630	A_{10}	510	1320	8	41	32	33	C	420
1230	A_{11}	510	1320	7	41	36	28	C	420
1830	A_{12}	510	1320	7	41	33	27	C	420
0030 26 Jan	A_{13}	510	1320	6	41	36	27	S	420
0630	A_{14}	510	1320	6	41	34	27	S	420
1230	B_1	370	750	5	40	35	22	S	960

TABLE 2 (Continued)

1830		B_2	360	800	5	41	32	20	S	960
0030	27 Jan	B_3	360	800	5	40	35	22	S	960
		C_1	400	1000	6	61	60	21	S	500
0630		B_4	360	800	6	40	32	25	C	960
		C_2	400	1000	6	61	58	22	S	500
1230		B_5	360	800	8	40	33	25	S	960
		C_3	400	1000	6	61	57	20	S	500
1830		B_6	360	800	6	40	33	21	S	960
		C_4	400	1000	5	61	58	20	S	500
0030	28 Jan	B_7	360	800	7	40	40	20	S	960
0630		B_8	360	800	7	40	40	20	S	960
1230		Effects no longer felt at Davenport during forecast period.								

[1] Determined by Geostrophic Wind Scale

[2] See Table 4

[3] S-straight, C-cyclonic, A-anticyclonic

TABLE 3

DATA COMPUTED FROM PARAMETERS OF TABLE 2

Fetch Desig.	Stab. Factor V_{gs}/V_g	Isobar Curv. Corr. I_{cc}	V_g Corr. to surface V_{gs}	Wind Used V	Fetch Limit F_L	Upper Period T_U	E	Equiv. During T_E (Hrs)	R_o	F_{LG}	$F-F_L$	Travel Time T_{ob} (Hrs)	Lower Per. T_L	Dur. Time T_D	Est. Time of Arrival ETA hr/day
A_1	.65	1	23	25	150	14.0	24	FD[1]	1620			76.5	3.9	FD[1]	03/26
A_2	.60	1	19	25	150	14.0	24	FD	1600			75.5	3.8	FD	10/26
A_3	.65	1	23	25	150	14.0	24	FD	1590			75.0	3.8	FD	15/26
A_4	.70	.95	27	25	150	14.0	24	FD	1590			75.0	3.8	FD	21/26
A_5	.70	.95	27	29	250	15.7	42	15.5	1490			62.5	4.5	21.5	15/26
A_6	.70	.95	30	34	350	17.0	78	19.0	1390			54.0	5.1	25.0	12/26
A_7	.60	1	27	32	400	18.4	94	FD	1340			48.0	5.8	FD	12/26
A_8	.65	1	29	34	500	18.7	110	FD	1240			44.0	6.3	FD	14/26
A_9	.65	.90	28	34	500	18.7	110	FD	1240			44.0	6.3	FD	20/26
A_{10}	.70	.95	33	34	500	18.7	110	FD	1240			44.0	6.3	FD	02/27
A_{11}	.70	.95	28	30	400	18.4	94	FD	1340			48.0	5.8	FD	12/27
A_{12}	.70	.95	27	30	300	16.7	58	FD	1440			57.0	4.8	FD	03/28
A_{13}	.70	1	27	30	300	16.7	58	FD	1440			57.0	4.8	FD	09/28
A_{14}	.70	1	27	30	300	16.7	58	FD	1440			57.0	4.8	FD	15/28

TABLE 3 (Continued)

B_1	.70	1	22	22	250	15.4	42	FD	1500	64.5	10.2	FD	04/29
B_2	.70	1	20	20	100	12.2	12	FD	1680	91.0	7.1	FD	13/30
B_3	.70	1	22	22	100	12.2	12	FD	1660	90.0	7.1	FD	18/30
C_1	.65	1	21	22	20	4.0	.7	FD	1480	200.0	--	3	--
B_4	.70	.95	25	25	150	13.3	20	FD	1600	80.0	7.9	FD	14/30
C_2	.65	1	22	22	25	8.5	80	3	1425	110.0	3.0	9	20/31
B_5	.70	1	25	28	200	14.7	3	FD	1560	70.0	9.0	FD	10/30
C_3	.65	1	20	22	100	12.2	12	FD	1400	76.0	4.3	FD	16/30
B_6	.70	1	21	24	200	14.7	15	FD	1560	70.0	9.0	FD	16/30
C_4	.65	1	20	22	100	12.2	12	FD	1400	76.0	4.3	FD	22/30
B_7	.65	1	20	28	200	15.2	15	FD	1560	68.0	9.3	FD	20/30
B_8	.65	1	20	28	250	15.7	16	FD	1510	64.0	9.9	FD	22/30

[1] Fully developed seas

TABLE 4

BEAUFORT WIND SPEED

Beaufort Number	Knots	Beaufort Number	Knots
1	1-3	7	28-33
2	4-6	8	34-40
3	7-10	9	41-47
4	11-16	10	48-55
5	17-21	11	56-65
6	22-27	12	Above 65

TABLE 5

STABILITY FACTORS

$\theta_s - \theta_a$	V_{gs}/V_g
<-7	0.55
-7 to 0	0.60
1 to 4	0.65
5 to 10	0.70
11 to 15	0.75
>15	0.80

Negative values of $\theta_s-\theta_a$ indicate stability, positive values indicate instability.

TABLE 6

ISOBAR CURVATURE CORRECTION

	Great Cyclonic	Moderate or Straight	Great Anticyclonic
Stable	$V_{gs} = 0.85V_g$	$V_{gs} = V_g$	$V_{gs} = 1.05V_g$
Indifferent	$V_{gs} = 0.90V_g$	$V_{gs} = V_g$	$V_{gs} = 1.1\ V_g$
Unstable	$V_{gs} = 0.95V_g$	$V_{gs} = V_g$	$V_{gs} = 1.15V_g$

TABLE 7

RELIABILITY OF POWER SPECTRUM ESTIMATES

f	Possible error in observed value				
	2.5 pct	5 pct	50 pct	95 pct	97.5 pct
1	1000	250	3.1	.26	.2
2	40	20	1.5	.33	.21
3	14	8.5	1.3	.36	.32
4	8.3	5.63	1.2	.42	.36
5	6.0	4.37	1.15	.46	.39
6	4.8	3.6	1.12	.48	.42
8	3.8	2.8	1.10	.51	.46
10	3.1	2.6	1.07	.55	.49
15	2.4	2.1	1.05	.60	.55
20	2.1	1.8	1.02	.63	.59
50	1.55	1.45	1.02	.74	.69
100	1.35	1.29	1.00	.79	.78
LARGE		$10^{1/\sqrt{f}}$		$10^{-1/\sqrt{f}}$	

TABLE 8

VALUES OF $[A(f)]^2$ AS A FUNCTION OF WIND SPEED (ft^2-sec)

Wind (knots)	$[A(f)]^2$																	
40	232	1012	3543	4820	4390	3365	2420	1685	1169	798	556	394	278	203	147	107	81	61
38	48.9	436	2100	3357	3330	2730	2060	1475	1044	729	515	367		192		103		60
36	.98	178	1182	2239	2500	2180	1730	1278	930	662	474	343		182		99		59
34		62.0	608	1434	1780	1685	1410	1085	806	590	429	315		170		94		55
32		18.8	267	794	1150	1208	1080	874	680	508	377	282		157		88.4		52
30		3.2	94.9	391	684	822	785	675	548	427		248		142		81.3		48.8
28		0.5	32.2	178	388	525	550	509	435	350	274	214		127		74.5		45.4
26			7.6	61.6	171	287	343	348	307	270	218	176		109		66.1		41.0
24			1.13	16.8	67.5	138.5	194	218	214	196	166	139		91		57.5		36.8
22				3.7	18.9	55.4	92.3	121	131.3	129.8	116.5	102.5	85.4	72.1		47.7		31.8
20					3.78	16.1	38.7	55.2	69.1	75.2	73.0	68.8	58.8	53.4	44.7	34.4	32.1	26.0
Freq.	.03	.04	.05	.06	.07	.08	.09	.10	.11	.12	.13	.14	.15	.16	.17	.18	.19	.20

BIBLIOGRAPHY

1. Sir H. Lamb, Hydrodynamics (6th edition), Cambridge University Press, Treatise on the Mathematical Theory of the Motion of Fluids, which was published in 1879.

2. V. Cornish, Ocean Waves and Kindred Geophysical Phenomena, Cambridge University Press, 163 p 1934.

3. F. E. Snodgrass, Operation Manual: Shore Wave Recorder, Mark IX, Model 5, University of California, Berkeley, Institute of Engineering Research, Tech. Report, Series 3, Issue 364, 42 pp plus illustrations, June 1954.

4. H. U. Sverdrup and W. H. Munk, Wind, Sea and Swell: Theory of Relations for Forecasting, U. S. Hydrographic Office, Pub. No. 601, 44 p 1947.

5. C. L. Bretschneider, Revised Wave Forecasting Curves and Procedure, University of California, Institute of Engineering Research, Berkeley, California, Series 29, No. 155-47, Sep 1951

6. J. W. Pierson, G. Neumann and R. W. James, Practical Methods for Observing and Forecasting Ocean Waves by Means of Wave Spectra and Statistics, U. S. Navy Hydrographic Office, Pub. No. 603.

7. R. L. Wiegel, Wave Transformation: Field Operations, Institute of Engineering Research, University of California, Series 29, Issue 56, Dec 1954.

8. W. J. Pierson and W. Marks, The Power Spectrum Analysis of Ocean-Wave Records, Transactions, American Geophysical Union, Vol. 33, No. 6, Dec 1952.

9. J. W. Tukey, and R. W. Hamming, Measuring Noise Color 1, Bell Telephone Laboratories, Murray Hill, New Jersey, 1949.

10. G. Neumann, Uber Seegang, Dunung und Wind (On Sea, Swell, and Wind), Deutsche Hydrographische Zeitschrift, Vol. 3, p 40-57, 1950.

11. M. S. Longuet-Higgins, On the Statistical Distribution of the Heights of Sea Waves, Journal of Marine Research, Vol. 11, p 245-266, 1952.

12. R. S. Arthur, W. H. Munk, and J. D. Isaacs, The Direct Construction of Wave Rays, Trans. A.G.U., Vol. 33, page 865, Dec 1952.

13. G. Neumann, On Interpretation of the Observable Properties of "Sea Waves" in Terms of the Energy Spectrum of the Gaussian Record, Transactions of the American Geophysical Union, Vol. 35, p 747-757, 1954.

14. R. C. Timme and F. A. Stinson, Preliminary Investigations on Predicting Properties of Bottom Pressure Fluctuations, U. S. Navy Hydrographic Office, TR-14.

15. Beach Erosion Board, An Ocean Wave Measuring Instrument, Corps of Engineers, Department of the Army, BEB Tech. Memo No. 6, 28 pp plus illustrations, Oct 1948.

16. M. V. Burt and M. Rattray, Jr., Comparison of Wave Forecasting Methods, Deep Sea Research V. I. pp 140, 1956.

17. S. Goldman, Information Theory, Prentice-Hall, Inc. 1953.

APPENDIX I

The purpose of this appendix is to tabulate values of $[A\ (f)]^2$ in Equation (1), Chapter 1, as a function of wind speed and frequency.

$$[A\ (f)]^2 = \frac{C}{(2\pi)^5 f^6}\ e^{-\frac{2g^2}{4\pi^2 f^2 v^2}} \qquad (1)$$

where $C = 4.8 \times 10^4\ cm^2\ sec^{-5}$

or $$[A\ (f)]^2 = \frac{5.27 \times 10^{-3}}{f^6}\ e^{\frac{-4.83 \times 10^4}{v^2 f^2}} \qquad (1a)$$

The values of the $[A(f)]^2$ for the solution of Equation (1a) are given in Table (8).

APPENDIX II

DESCRIPTION OF LOCALE AND FACILITIES AT THE FORECAST SITE, DAVENPORT, CALIFORNIA

The University of California, with the permission of Santa Cruz Portland Cement Company, planned, established, and maintained an ocean wave recording program at Davenport, California. As shown in Figure 15, the pier extended twenty-two hundred feet seaward of the beach and was exposed to the large waves from the North Pacific generating areas. Elaborate instrumentation and recording devices were used. Continuous ocean wave records from 8 Nov 1952 to 1 Dec 1954 were obtained from the Beach Erosion Board (BEB), step-resistor gages (parallel type) [15] and Mark IX [3] pressure heads. The locations of these two instruments are shown in Figure 13. The BEB was located at the seaward end of the pier. Depth immediately below the BEB was 50 feet. The Mark IX was located in $81\frac{1}{2}$ feet of water (below MLLW).

Fluctuations of the sea surface were transferred by electrical circuitry to a recording center located on shore. Here the fluctuations were permanently recorded on Esterline-Angus Continuous Record Charts.[1] Two time scales were used:

6" per 1 minute, called "fast time"

6" per 1 hour, called "slow time"

Fast time was recorded every twelve hours for twenty minutes beginning at 0430Z and 1630Z of each day. t_i (forecast time)was determined by the fast time records.

A continual maintenance schedule was kept, which involved mainly cleaning and re-calibration.

[1]See Figure 21

APPENDIX III

DESCRIPTION OF THE SYNOPTIC SITUATION DURING AND PRECEDING THE FORECAST TIME

As explained in Chapter 3, the forecast time began at 0430Z, 28 Jan 1954 and ended at 0430Z, 1 Feb 1954.

The synoptic situation affecting the forecast locality during and preceding the forecast time remained basically stationary. A low pressure center (average 1000 MB) existed over the Gulf of Alaska or British Columbia from 1230Z, 22 Jan 1954 to 1230Z, 28 Jan 1954. A strong high pressure center (1040 MB) maintained itself over Alaska and the Bering Sea with a ridge extending southeastward down to 35 N latitude. Figure 7 illustrates the general synoptic situation that existed before and remained nearly constant during the forecast period.

The large cyclonic circulation in the Gulf of Alaska created a fetch of length (F_{LG}) 1320 nautical miles. Fetch width (F_W) was 520 nautical miles with the distance from the center of the leeward side to Davenport (R_o) being 420 nautical miles. This fetch hereafter will be referred to as Fetch "A." Fetch A existed fully developed from 0030Z, 23 Jan 1954 to 0630Z, 26 Jan 1954.

At approximately 0630Z, 26 Jan 1954, due to a slight reorientation of the cyclonic circulation, F_{LG} became 800 nautical miles with a corresponding increase in R_o to 960 nautical miles. This change resulted in a redesignation to Fetch "B." All other geographic variables remained constant. Fetch B existed from 0630Z, 26 Jan 1954 to 1230Z, 28 Jan 1954.

Data for fetches A and B were recorded in Table 2, Chapter 3, and the fetches are illustrated in Figure 7.

Wind is one of the most important variables in forecasting an energy

spectrum. The general wind area remained fairly constant but wind varied before and during the forecast period in fetches A and B. The variation of the average wind speed with time in fetches A and B is illustrated in Figure 17.

Figure 8 illustrates the general synoptic situation that existed from 0030Z, 27 Jan 1954 to 1830Z, 27 Jan 1954. A fetch, Fetch C, was fitted to this circulation. Data resulting from this fetch are recorded in Table 2, Chapter 3.

The wind field remained constant at 22 knots during the existence of Fetch C.

Fetch A existed for 84 hours, B for 48 hours, and C for 18 hours. The subscript notation (A_i,B_i,C_i) was used to distinguish fetch sequence, with a map interval of 6 hours. The fetch life started when i = 1, and ended when i = 14, i = 8, and i = 4 respectively.

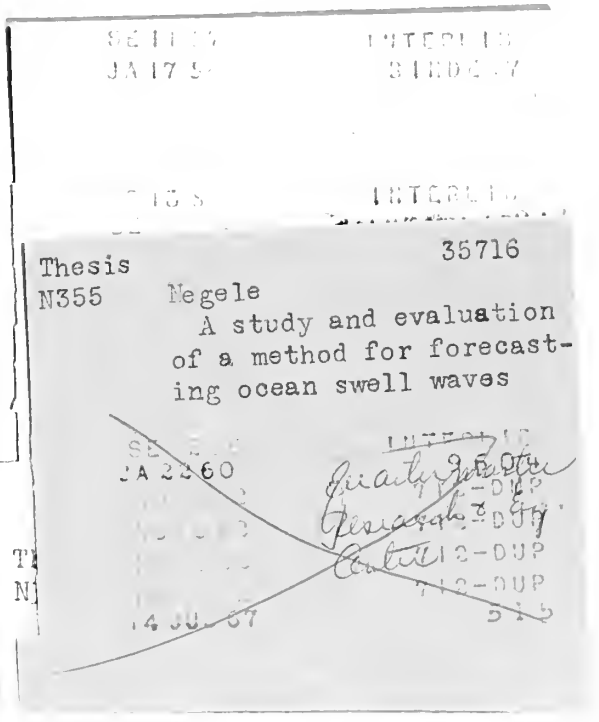

Thesis
N355 Negele
A study and evaluation of a method for forecasting ocean swell waves using wave spectra.